

Supporting Information

New design rules for developing potent, cell-active inhibitors of the Nucleosome Remodeling Factor (NURF) via BPTF bromodomain inhibition

Huda Zahid,^{‡,a} Caroline R. Buchholz,^{‡,b} Manjulata Singh,^c Michael F. Ciccone,^d Alice Chan,^e Stanley Nithianantham,^f Ke Shi,^g Hideki Aihara,^g Marcus Fischer,^f Ernst Schonbrunn,^e Camila O. dos Santos,^d Joseph W. Landry,^c William C. K. Pomerantz^{*,a,b}

^aDepartment of Chemistry, University of Minnesota, 207 Pleasant St. SE, Minneapolis, Minnesota 55455, United States

^bDepartment of Medicinal Chemistry, University of Minnesota, 308 Harvard Street SE, Minneapolis, Minnesota 55455, United States

^cThe Department of Human and Molecular Genetics, VCU Institute of Molecular Medicine, Massey Cancer Center, Virginia Commonwealth University, Richmond, Virginia 23298, United States

^dCold Spring Harbor Laboratory, 1 Bungtown Road, Cold Spring Harbor, NY 11724, United States

^eDrug Discovery Department, H. Lee Moffitt Cancer Center and Research Institute, 12902 Magnolia Drive, Tampa, Florida 33612, United States

^fDepartment of Chemical Biology & Therapeutics, St. Jude Children's Research Hospital, Memphis, TN 38105, United States; and Department of Structural Biology, St. Jude Children's Research Hospital, Memphis, TN 38105, United States

^gDepartment of Biochemistry, Molecular Biology, and Biophysics, University of Minnesota, 321 Church St. SE, Minneapolis, Minnesota 55455, United States

[‡]These authors contributed equally to the manuscript.

Corresponding Author: *William C.K. Pomerantz, email: wcp@umn.edu

Contents

PrOF NMR titration of 4,5-dichloropyridazinone with 5FW-BPTF	2
AlphaScreen titrations of small molecules	2
Cocrystal structures of BPTF with compounds 1-4 and 11	4
Solubility tests for compounds 18 (BZ1), 19 and 20 in PBS	7
BROMOScan data	8
Cell culture data	11
Analytical HPLC traces of compounds 18-20	14
X-ray Crystallography statistics	14
¹H and ¹³C NMR spectra of small molecule analogues	18
References	43

No unexpected or unusually high safety hazards were encountered in the experimental methods used for this manuscript.

PrOF NMR titration of 4,5-dichloropyridazinone with 5FW-BPTF

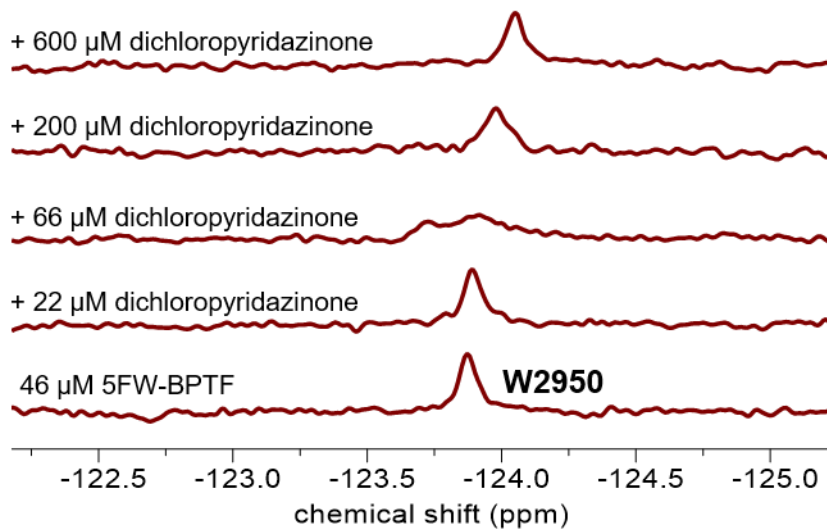


Figure S1: PrOF NMR titration of 4,5-dichloropyridazinone with 5FW-BPTF.

AlphaScreen titrations of small molecules

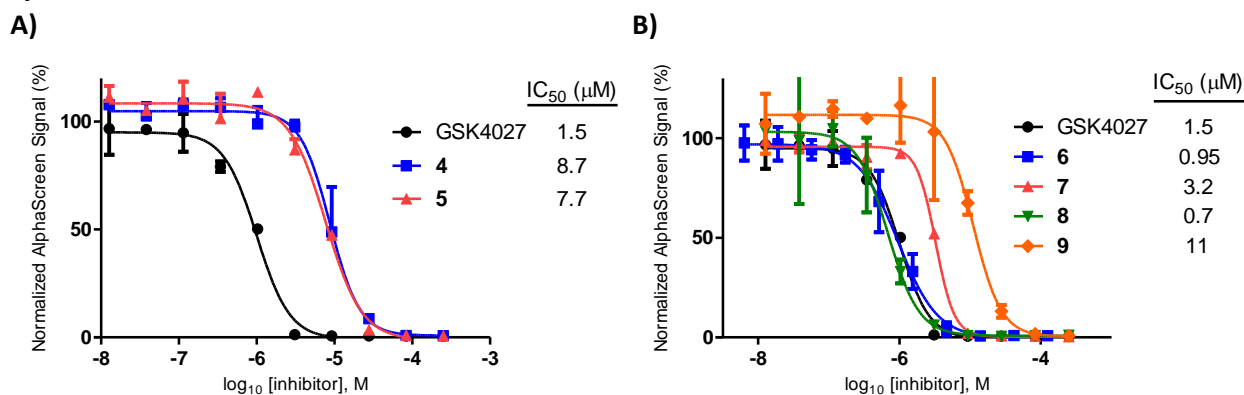


Figure S2: AlphaScreen titration of BPTF with compounds from **A)** Table 1 and **B)** Table 2

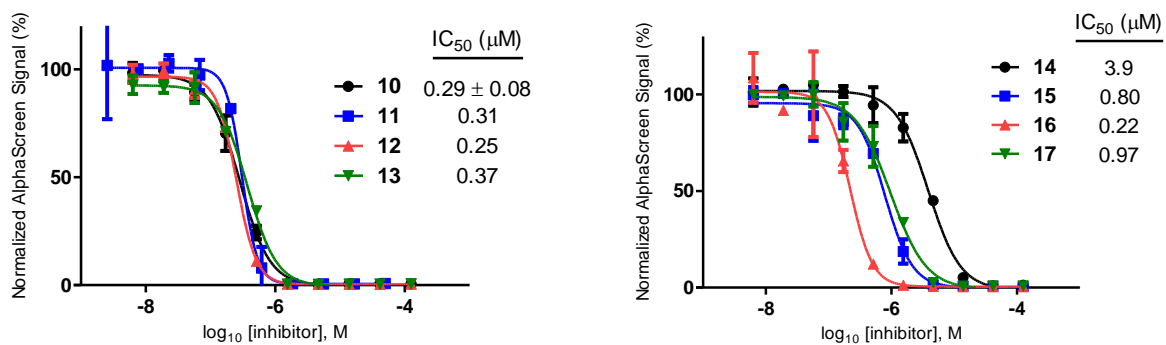


Figure S3: AlphaScreen titration of BPTF with compounds from Table 3

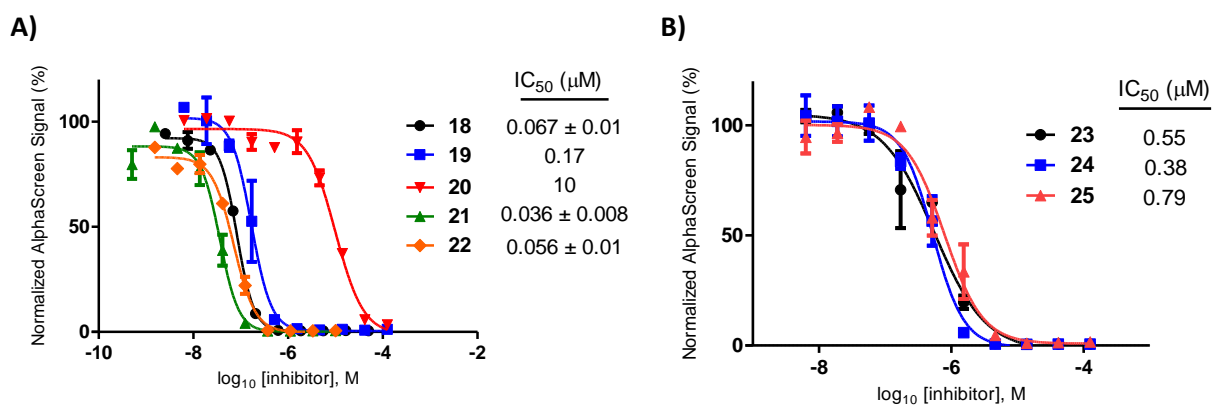


Figure S4: AlphaScreen titration of BPTF with compounds from A) Table 4 and B) Table 5

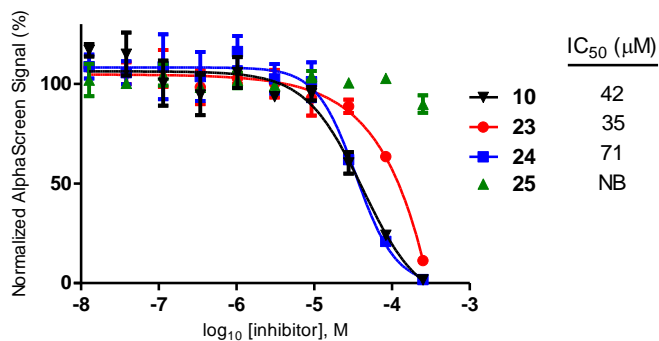


Figure S5: AlphaScreen titration of BRD4 D1 with compounds from Table 5

Cocrystal structures of BPTF with compounds 1-4 and 11

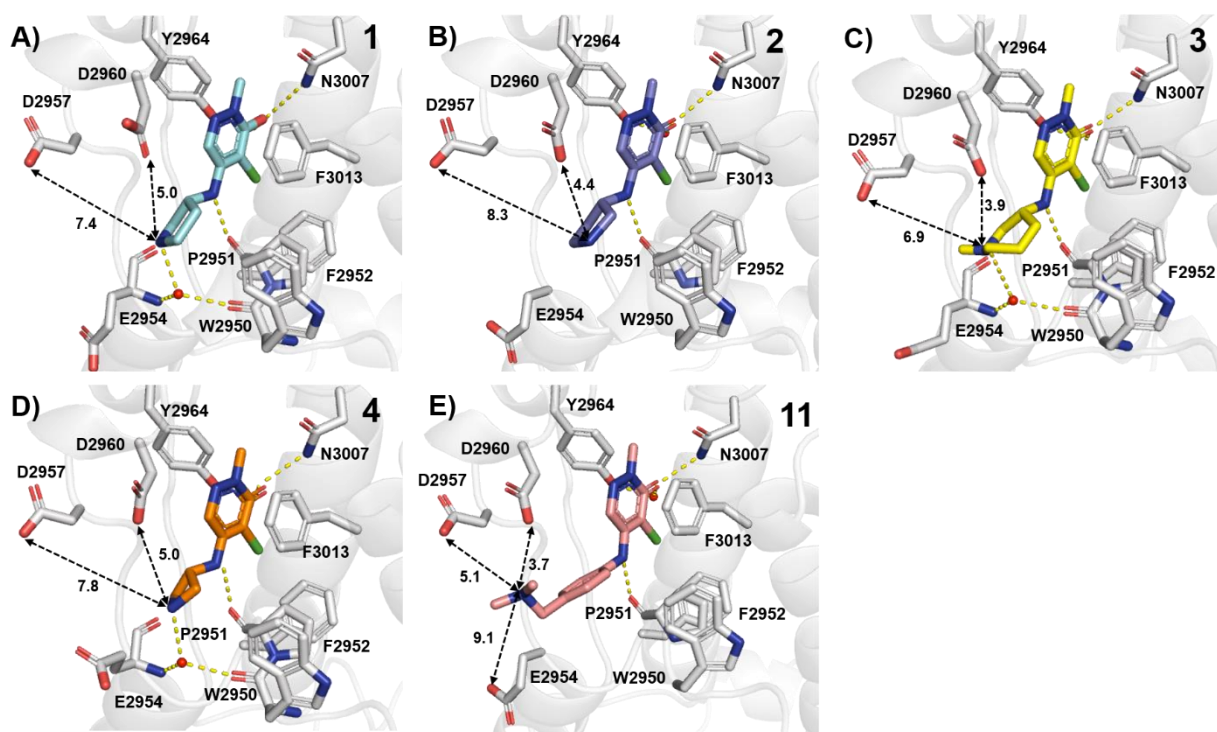
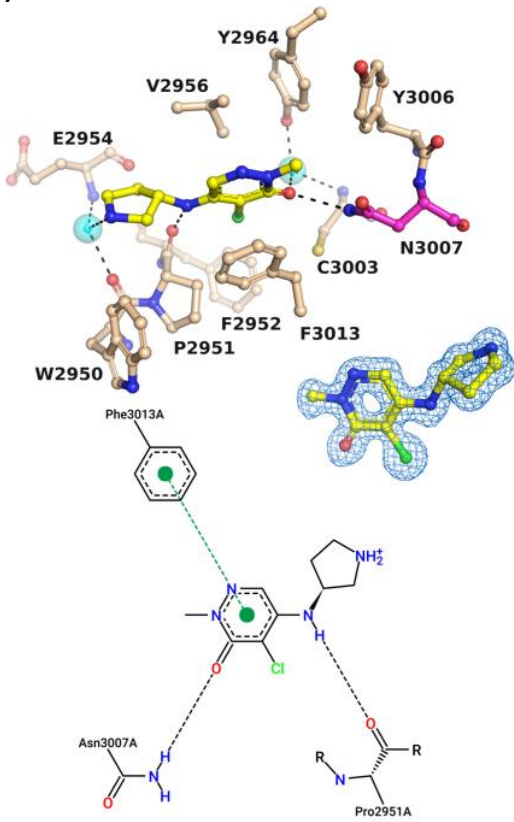
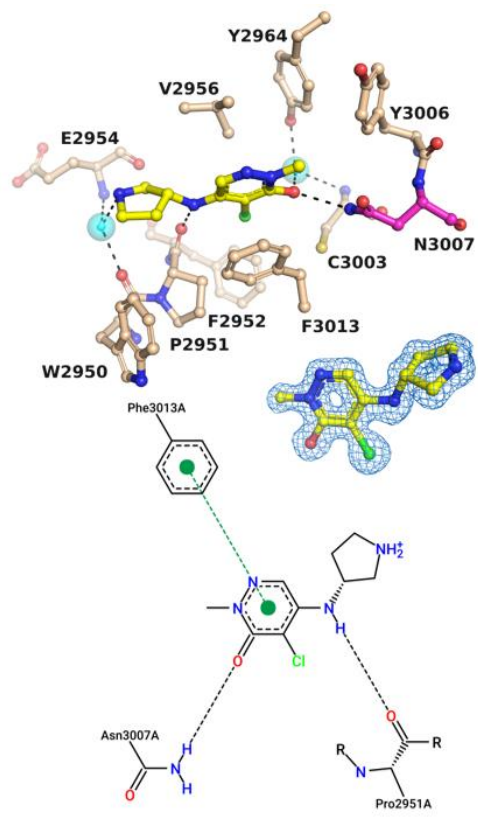


Figure S6: BPTF bromodomain (gray) cocrystal structures with **A) 1** (PDB: 7LPK, 1.39 Å resolution), **B) 2** (PDB: 7LRK, 1.44 Å resolution), **C) 3** (PDB: 7LPO, 1.66 Å resolution), **D) 4** (PDB: 7LRO, 1.45 Å resolution) and **E) 11** (PDB: 7RWN, 1.39 Å resolution). Hydrogen bonds are shown as yellow dashed lines. The distances (Å) between key residues are indicated. Three of the conserved structured waters are excluded for clarity.

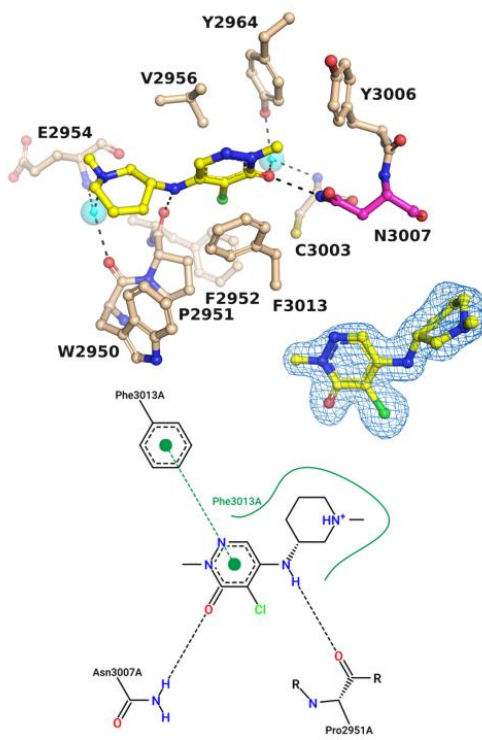
A)



B)



C)



D)

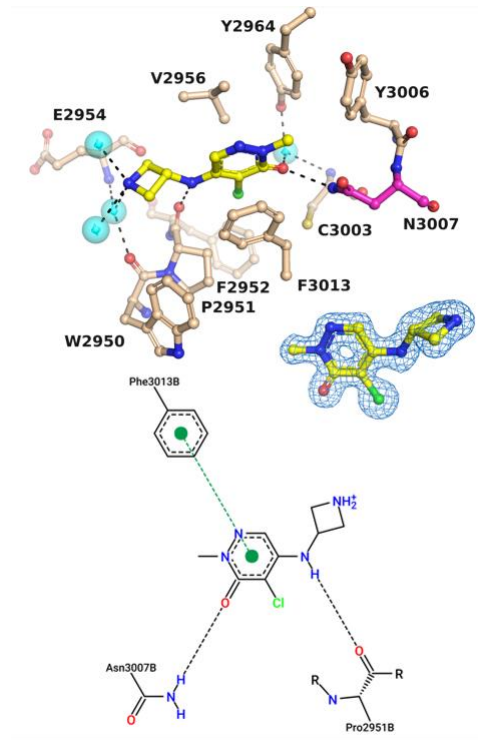


Figure S7: BPTF bromodomain (beige) cocrystal structures with small molecules **A) 1** (PDB: 7LPK, 1.39 Å resolution), **B) 2** (PDB: 7LRK, 1.44 Å resolution), **C) 3** (PDB: 7LPO, 1.66 Å resolution) and **D) 4** (PDB: 7LRO, 1.45 Å resolution) in yellow. Bound waters indicated by cyan spheres. Blue mesh around the inhibitor shows the corresponding 2Fo-Fc electron density map contoured at 1σ . Water-mediated H-bonds are excluded from the interaction schematics for clarity.

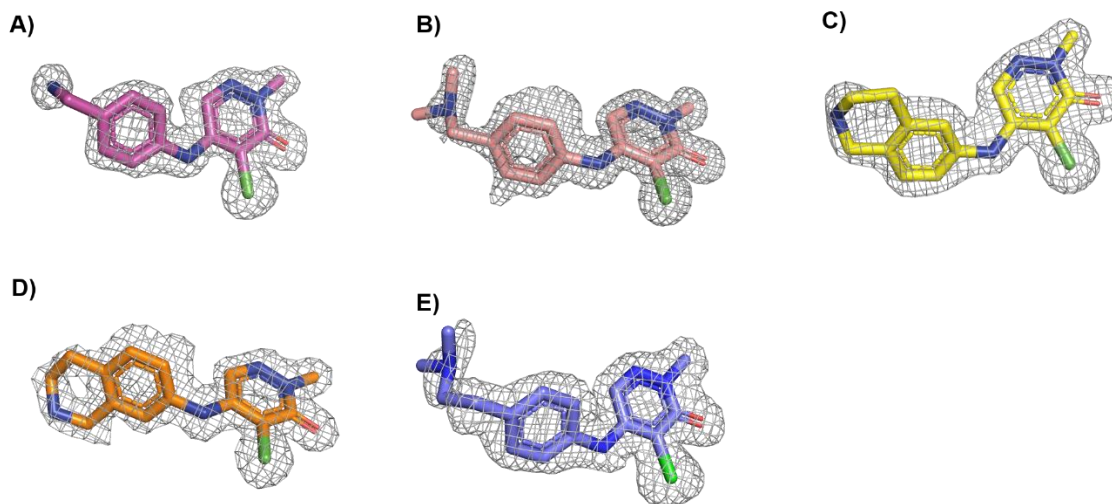


Figure S8: BPTF bromodomain (gray) cocrystal structures with **A) 10** (PDB: 7RWP), **B) 11** (PDB: 7RWN), **C) 12** (PDB: 7RWQ), **D) 13** (PDB: 7RWO), and **E) 19** (PDB: 7M2E). Gray mesh around the ligand shows the corresponding 2Fo-Fc electron density map contoured at 1σ .

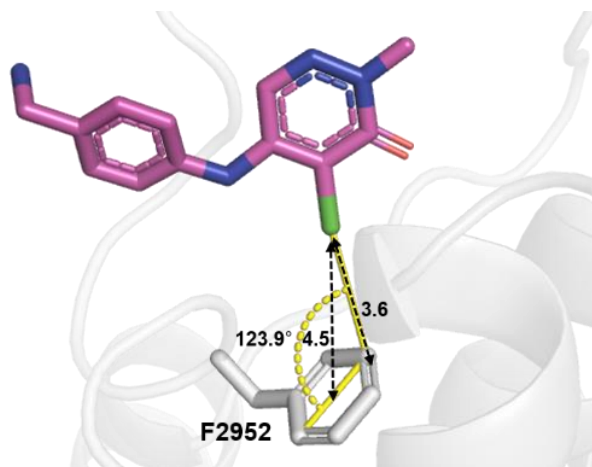


Figure S9: BPTF bromodomain (gray) cocrystal structure with **10**. The distances between the chlorine on **10** and the aromatic ring of F2952 are indicated, as well as the angle between chlorine and the ring plane. (PDB: 7RWP, 1.73 Å resolution).

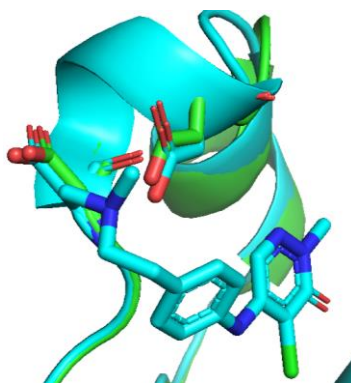
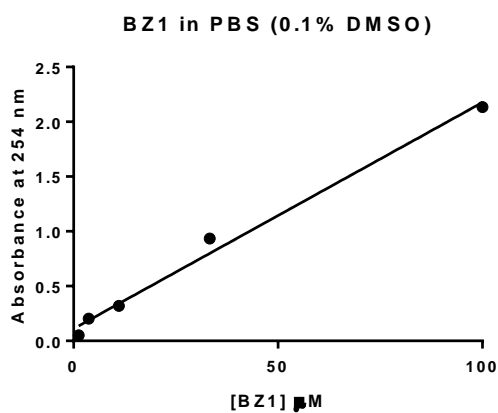


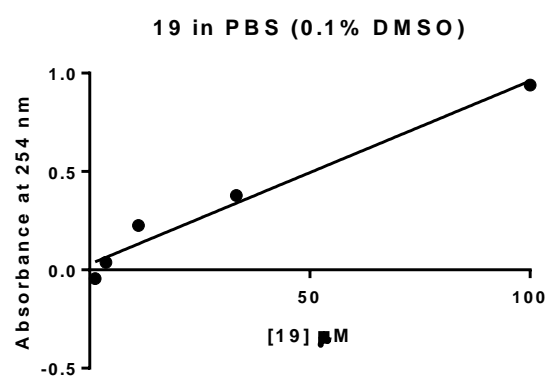
Figure S10: Overlay of apo structure of BPTF (PDB: 3UV2, green) with **19** (PDB: 7M2E, cyan).

Solubility tests for compounds **18** (BZ1), **19** and **20** in PBS

A)



B)



C)

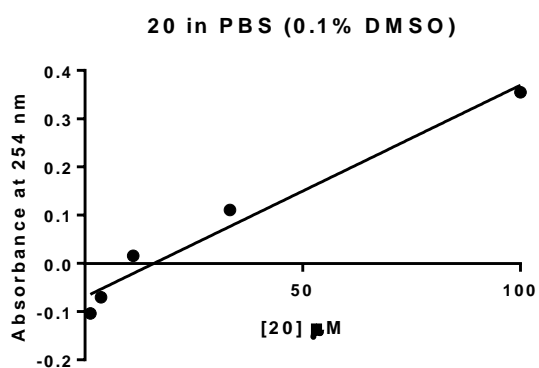
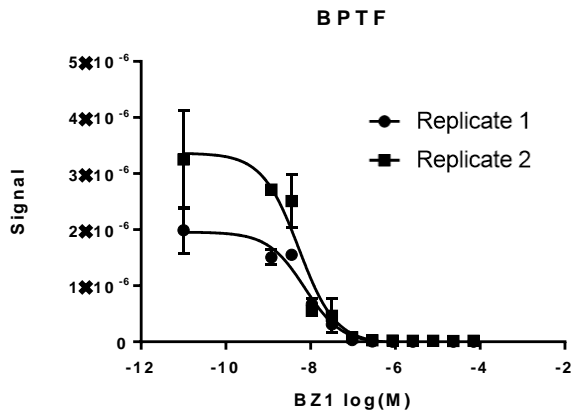


Figure S11: Solubility test by UV-Vis of compounds **A) BZ1**, **B) 19**, **C) 20** up to 100 μM in 0.1% DMSO in Phosphate Buffered Saline (PBS) at 254 nm.

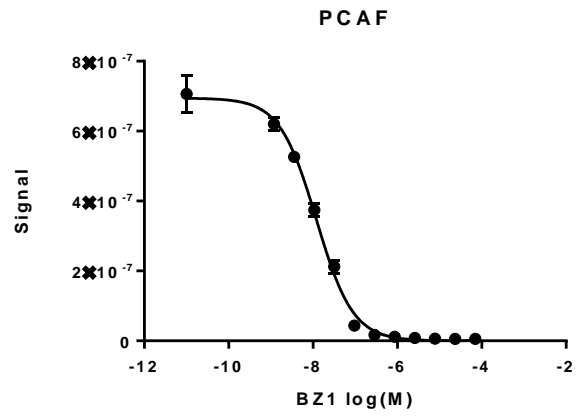
BROMOscan dataTable S1: BROMOscan single point measurements at 140 nM **18 (BZ1)**

DiscoverX Gene Symbol	Entrez Gene Symbol	Percent Control
ATAD2A	ATAD2	53
ATAD2B	ATAD2B	73
BAZ2A	BAZ2A	63
BAZ2B	BAZ2B	38
BRD1	BRD1	24
BRD2(1)	BRD2	100
BRD2(2)	BRD2	65
BRD3(1)	BRD3	50
BRD3(2)	BRD3	89
BRD4(1)	BRD4	29
BRD4(2)	BRD4	63
BRD7	BRD7	1.1
BRD9	BRD9	1.3
BRDT(1)	BRDT	97
BRDT(2)	BRDT	66
BRPF1	BRPF1	10
BRPF3	BRPF3	41
CECR2	CECR2	5.7
CREBBP	CREBBP	57
EP300	EP300	51
FALZ	BPTF	0
GCN5L2	KAT2A	34
PBRM1(2)	PBRM1	97
PBRM1(5)	PBRM1	100
PCAF	KAT2B	0
SMARCA2	SMARCA2	88
SMARCA4	SMARCA4	85
TAF1(2)	TAF1	34
TAF1L(2)	TAF1L	69
TRIM24(PHD,Bromo.)	TRIM24	81
TRIM33(PHD,Bromo.)	TRIM33	58
WDR9(2)	BRWD1	88

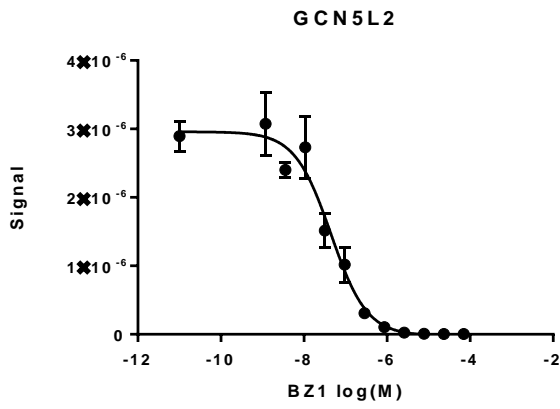
A)



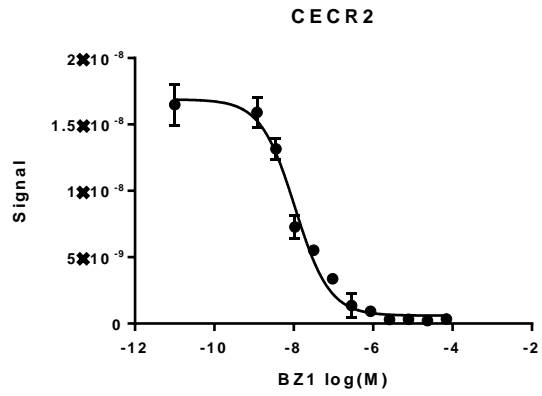
B)



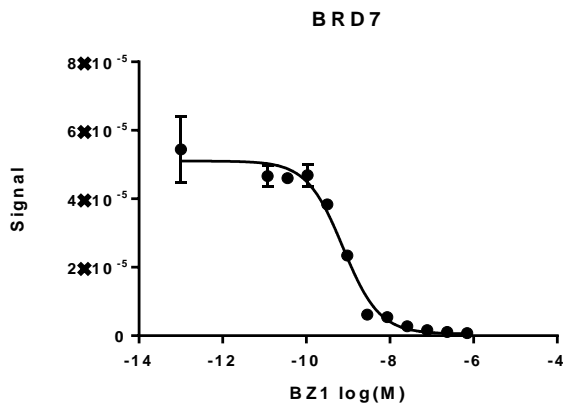
C)



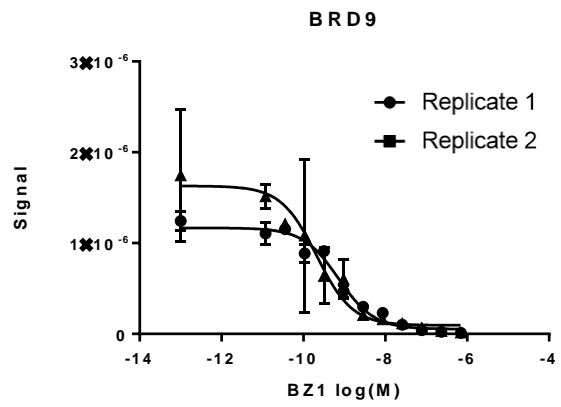
D)



E)



F)



G)

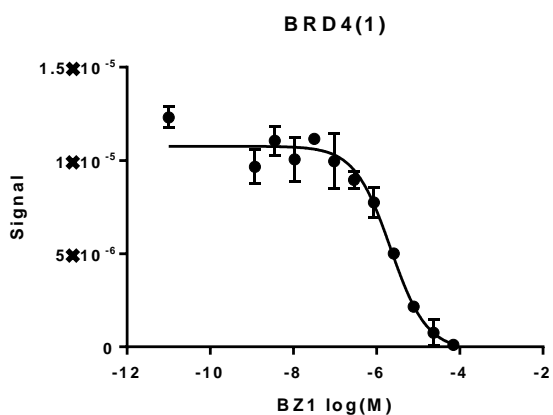
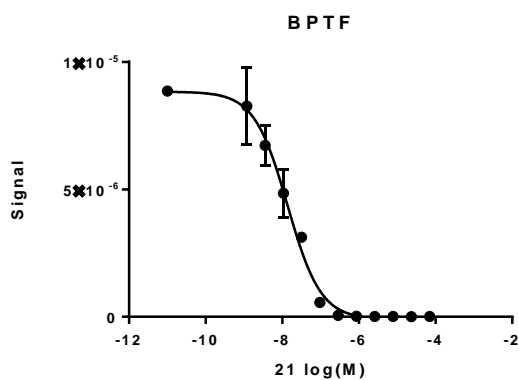
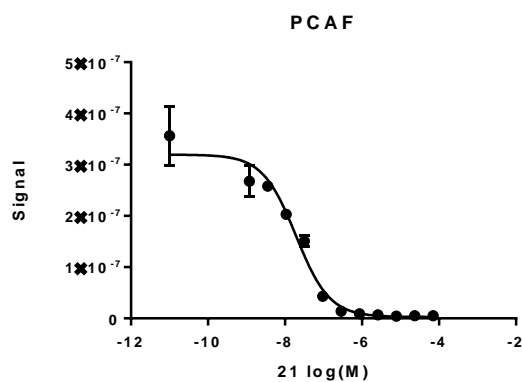


Figure S12: DiscoverX BROMOscan titrations of **BZ1** with **A)** BPTF, **B)** PCAF, **C)** GCN5L2, **D)** CECR2, **E)** BRD7, **F)** BRD9 and **G)** BRD4 (1). Annotations replicate 1 and 2 in the graph legend indicate the two experimental replicates.

A)



B)



C)

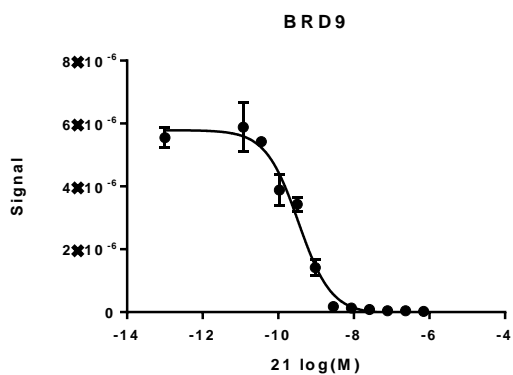
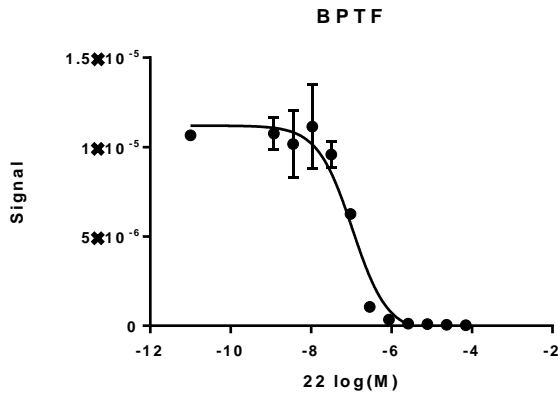
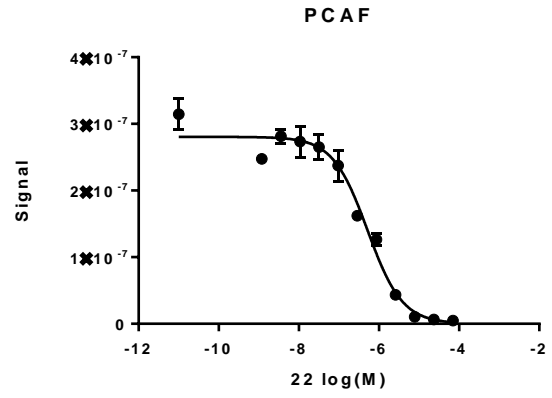


Figure S13: DiscoverX BROMOscan titrations of **21** with **A)** FALZ (BPTF) **B)** PCAF and **C)** BRD9 bromodomains.

A)



B)



C)

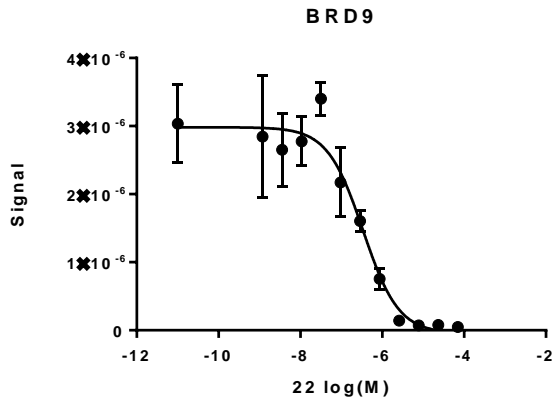
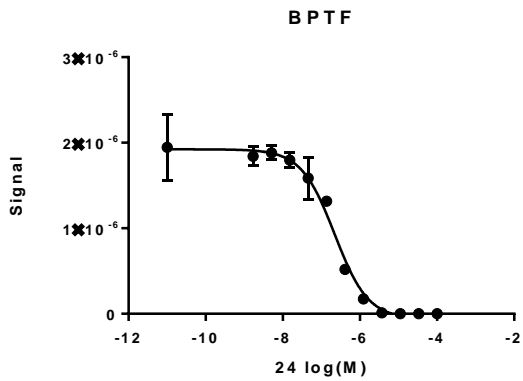


Figure S14: DiscoverX BROMOScan titrations of **22** with **A)** FALZ (BPTF) **B)** PCAF and **C)** BRD9 bromodomains.

A)



B)

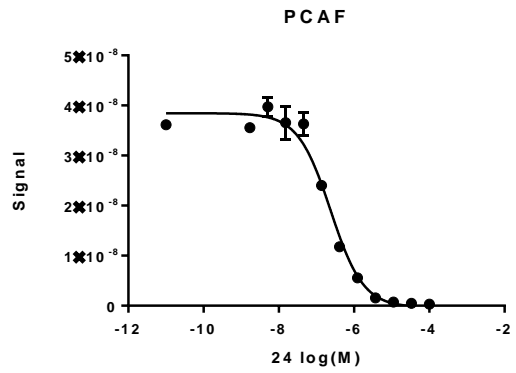


Figure S15: DiscoverX BROMOScan titrations of **24** with **A)** FALZ (BPTF) and **B)** PCAF bromodomains.

Cell culture data

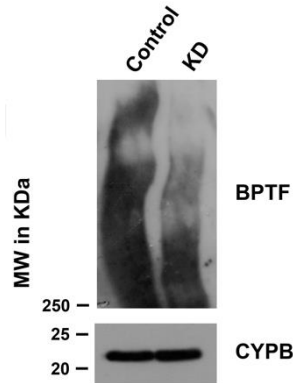


Figure S16: Western blot showing BPTF KD in 4T1 cells, methods previously reported by Mayes et al.¹

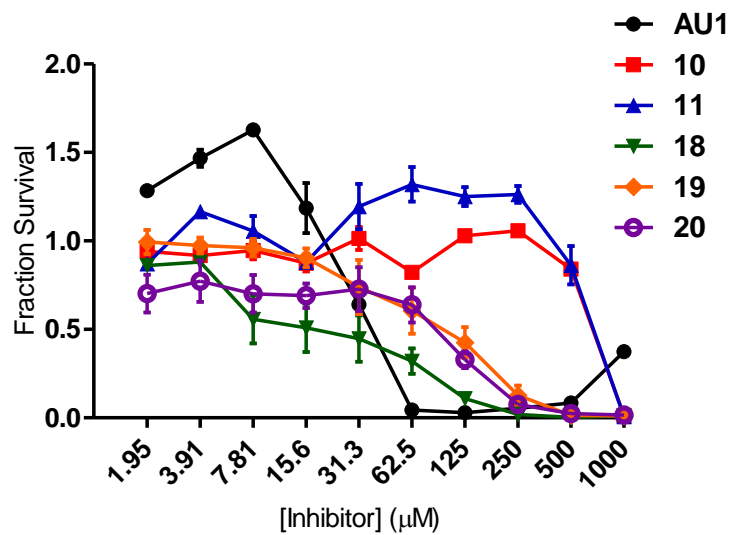


Figure S17: MTS assay with AU1 and pyridazinone inhibitors **10**, **11**, **18 (BZ1)**, **19** and **20**.

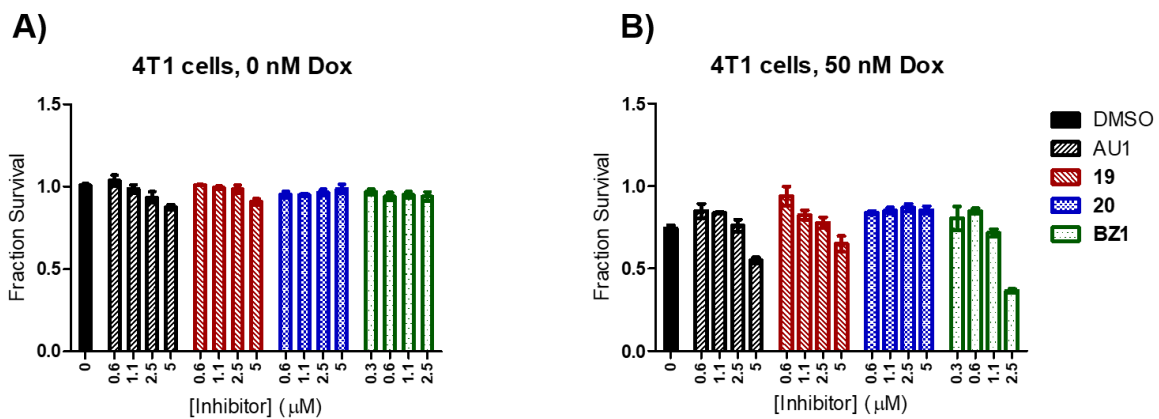


Figure S18: 4T1 cells were tested with AU1 and pyridazinone inhibitors **19**, **20** and **BZ1** at lower concentrations than in Figure 6. **A)** without doxorubicin **B)** in the presence of 50 nM doxorubicin. Fraction survival values are averages of three experimental replicates, except DMSO controls which are averages of nine experimental replicates.

Table S2: RNA-seq data from prior BPTF KO studies²

Gene	fold-change	p-value
<i>Sfn</i>	11.47661989	1.42E-05
<i>Sprr1a</i>	7.587300464	0.000137877
<i>Myc</i>	2.255253239	0.093807516

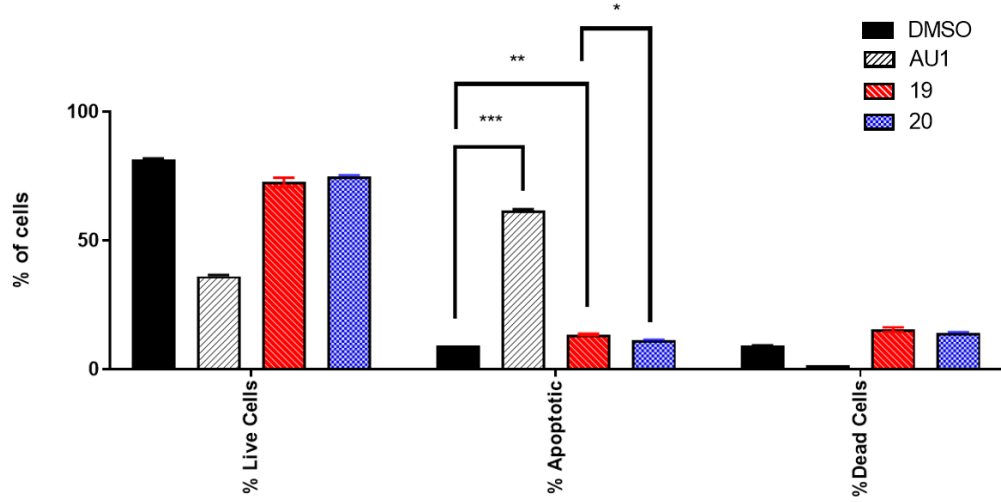


Figure S19: Viability analysis of Eph4 cells treated with 5 μ M compound or DMSO

DMSO vs AU1: $p = .0001$

19 vs 20: $p = .0253$

DMSO vs 19: $p = .0042$

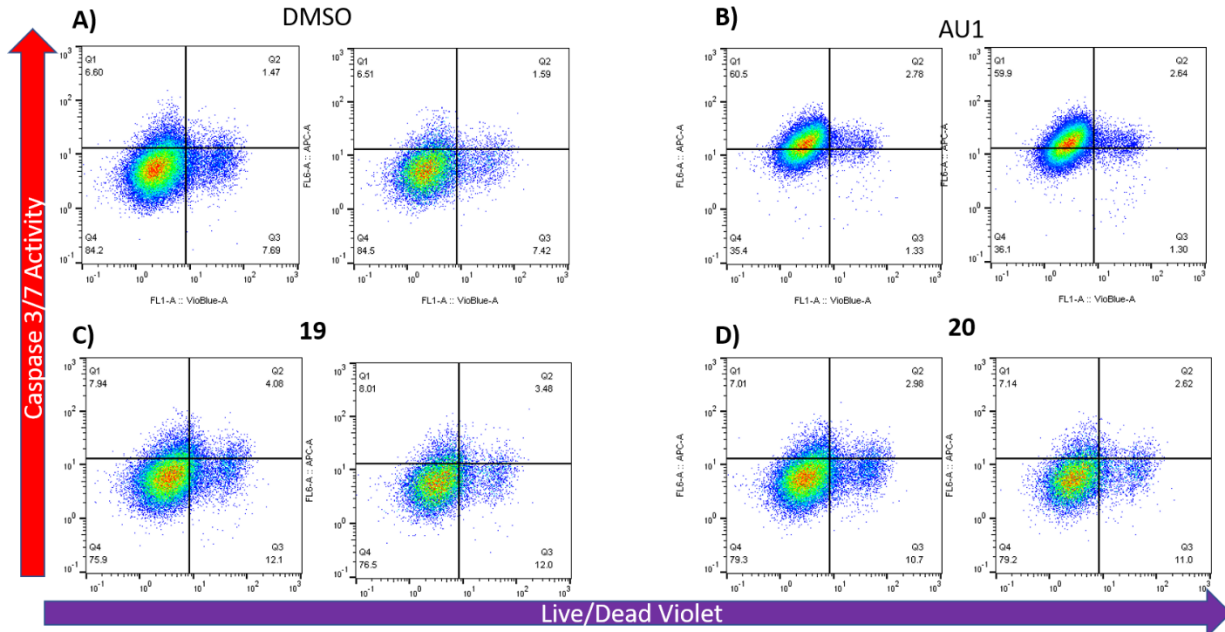


Figure S20: Caspase activation and viability analysis of Eph4 cells treated with 5 μ M compound or DMSO

Analytical HPLC traces of compounds 18-20

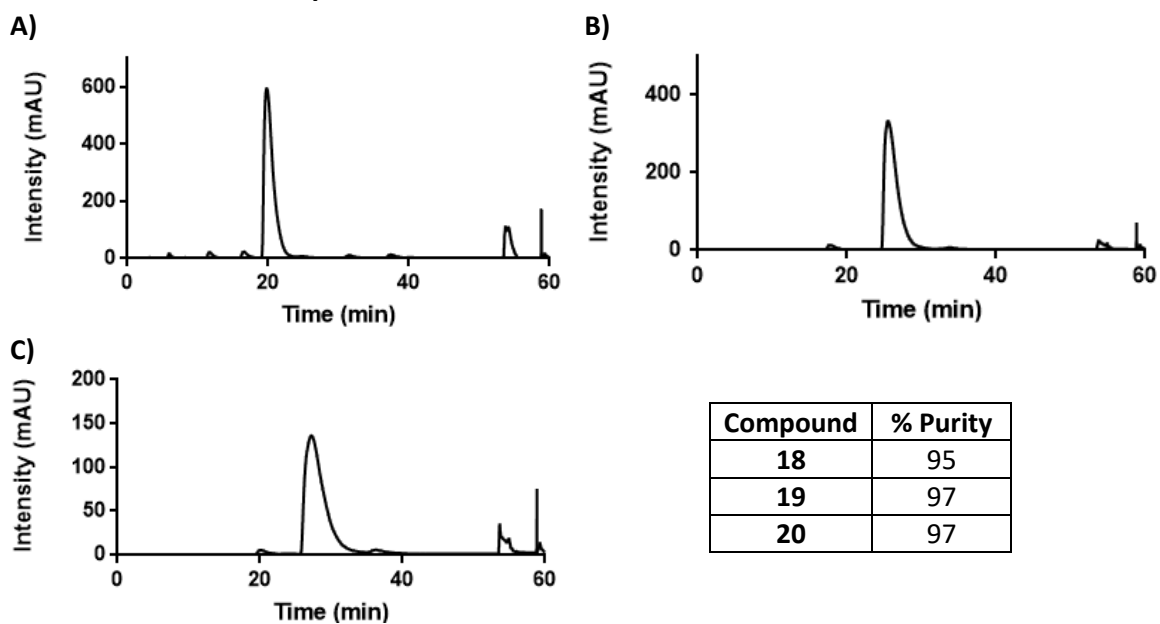


Figure S21: HPLC spectra at 272 nm of **A) 18**, **B) 19**, and **C) 20** over a gradient of 0-10% ACN in H₂O with a calculated % purity from 0-50 min (excluding the solvent front).

X-ray Crystallography statistics

Table S3: Data collection and refinement statistics for compounds 1-4

Inhibitor		3	1	2	4
PDB ID		7LP0	7LPK	7LRK	7LRO
Data collection					
Space group		P1	P2 ₁	P2 ₁	P2 ₁
Unit cell dimensions	a	27.1	58.4	58.3	58.4
	b	35.6	27.2	27.1	27.1
	c	57.6	76.9	76.7	76.9
	α	97.1	90.0	90.0	90.0
	β	103.6	93.7	93.7	93.9
	γ	94.3	90.0	90.0	90.0
Resolution range (Å)		38.0 - 1.66 (1.70 - 1.66)	38.4 - 1.39 (1.43 - 1.39)	38.3 - 1.44 (1.48 - 1.44)	38.1 - 1.45 (1.49 - 1.45)
Unique reflections		25204 (1843)	48967 (3673)	43465 (2851)	43259 (3165)
Rmeas (%)		10.9 (65.2)	7.3 (58.5)	7.1 (45.3)	8.2 (58.6)
CC1/2 (%)		99.3 (67.2)	99.8 (74.4)	99.8 (87.6)	99.8 (78.2)
Completeness (%)		94.7 (91.3)	99.2 (99.8)	98.3 (88.1)	99.8 (99.7)
I/σI		10.6 (3.0)	14.1 (3.4)	16.7 (3.6)	14.0 (2.5)
Structure refinement					
Rwork (%)		19.1 (33.3)	19.0 (24.9)	16.6 (22.6)	15.9 (21.5)
Rfree^a (%)		23.5 (41.8)	20.4 (33.3)	18.8 (26.5)	19.1 (25.3)
Wilson B (Å²)		22.7	9.8	8.7	9.2
Average B (Å²)	all	27.8	13.5	11.7	13.6
	protein	27.5	12.5	10.5	11.6
	ligand	27.6	12.4	10.1	11.6
	solvent	31.7	21.2	19.7	24.1
rmsd^b bond lengths (Å)		0.006	0.005	0.006	0.005
rmsd bond angles (deg)		0.84	0.76	0.82	0.83
Ramachandran	favoured (%)	98.65	100	100	100
	allowed (%)	1.35	0.0	0.0	0.0
	outliers (%)	0.0	0.0	0.0	0.0

Values in parenthesis are for the highest resolution bins.

^a Rfree is Rcryst calculated for randomly chosen unique reflections.

^b rmsd = root-mean-square deviation from ideal values.

Table S4: Data collection and refinement statistics for compounds **10-13**.

	10	11	12	13
PDB ID	7RWP	7RWN	7RWQ	7RWO
Resolution range	48.31 - 1.73 (1.792 - 1.73)	38.28 - 1.39 (1.44 - 1.39)	35.61 - 1.9 (1.968 - 1.9)	33.32 - 1.58 (1.636 - 1.58)
Space group	P 2 21 21	P 1 21 1	P 2 21 21	P 1 21 1
Unit cell	27.131 66.337 70.506 90 90 90	27.148 66.854 39.706 90	27.18 66.346 71.216	27.098 66.638 39.288 90

		105.406 90	90 90 90	106.787 90
Total reflections	62016 (6463)	100196 (9373)	74932 (7559)	64535 (6691)
Unique reflections	13659 (1383)	27024 (2710)	10647 (1044)	17736 (1788)
Multiplicity	4.5 (4.7)	3.7 (3.5)	7.0 (7.2)	3.6 (3.7)
Completeness (%)	98.08 (99.64)	98.18 (98.44)	99.31 (99.71)	96.46 (98.24)
Mean I/sigma(I)	10.69 (2.14)	11.04 (2.57)	9.43 (2.04)	9.37 (2.08)
Wilson B-factor	17.42	11.59	20.6	14.60
R-merge	0.1015 (0.6784)	0.07337 (0.4816)	0.1636 (0.9022)	0.1067 (0.5826)
R-meas	0.114 (0.7611)	0.08561 (0.5697)	0.1767 (0.9711)	0.1265 (0.6807)
R-pim	0.05057 (0.3354)	0.04341 (0.2992)	0.06546 (0.3538)	0.06649 (0.3465)
CC1/2	0.998 (0.783)	0.997 (0.762)	0.994 (0.666)	0.934 (0.737)
CC*	0.999 (0.937)	0.999 (0.93)	0.999 (0.894)	0.983 (0.921)
Reflections used in refinement	13659 (1383)	27024 (2708)	10646 (1043)	17736 (1787)
Reflections used for R- free	1358 (137)	1985 (209)	1073 (106)	1771 (184)
R-work	0.2208 (0.2587)	0.1885 (0.2552)	0.2155 (0.3032)	0.1965 (0.2920)
R-free	0.2693 (0.3355)	0.2133 (0.3002)	0.2575 (0.3559)	0.2278 (0.3213)
CC(work)	0.942 (0.873)	0.955 (0.852)	0.948 (0.744)	0.930 (0.759)
CC(free)	0.911 (0.772)	0.941 (0.831)	0.880 (0.725)	0.835 (0.732)
Number of non- hydrogen atoms	1052	1140	1056	1109
macromolecules	983	1008	996	1019
ligands	19	20	21	20
solvent	50	112	39	70
Protein residues	117	120	119	120
RMS(bonds)	0.007	0.007	0.008	0.006
RMS(angles)	1.12	0.93	1.01	0.78
Ramachandran favored (%)	100.00	99.15	99.14	99.15
Ramachandran allowed (%)	0.00	0.85	0.86	0.85
Ramachandran outliers (%)	0.00	0	0	0.00
Rotamer outliers (%)	0.00	0	0.88	2.59
Clashscore	2.04	0.99	4.02	2.45
Average B-factor	18.69	14.93	22.14	16.32
macromolecules	18.46	14.17	22.15	16.09
ligands	26.57	19.51	23.17	17.37

solvent	20.11	20.9	21.23	19.49
---------	-------	------	-------	-------

Statistics for the highest-resolution shell are shown in parentheses.

Table S5: Data collection and refinement statistics for compound **19**.

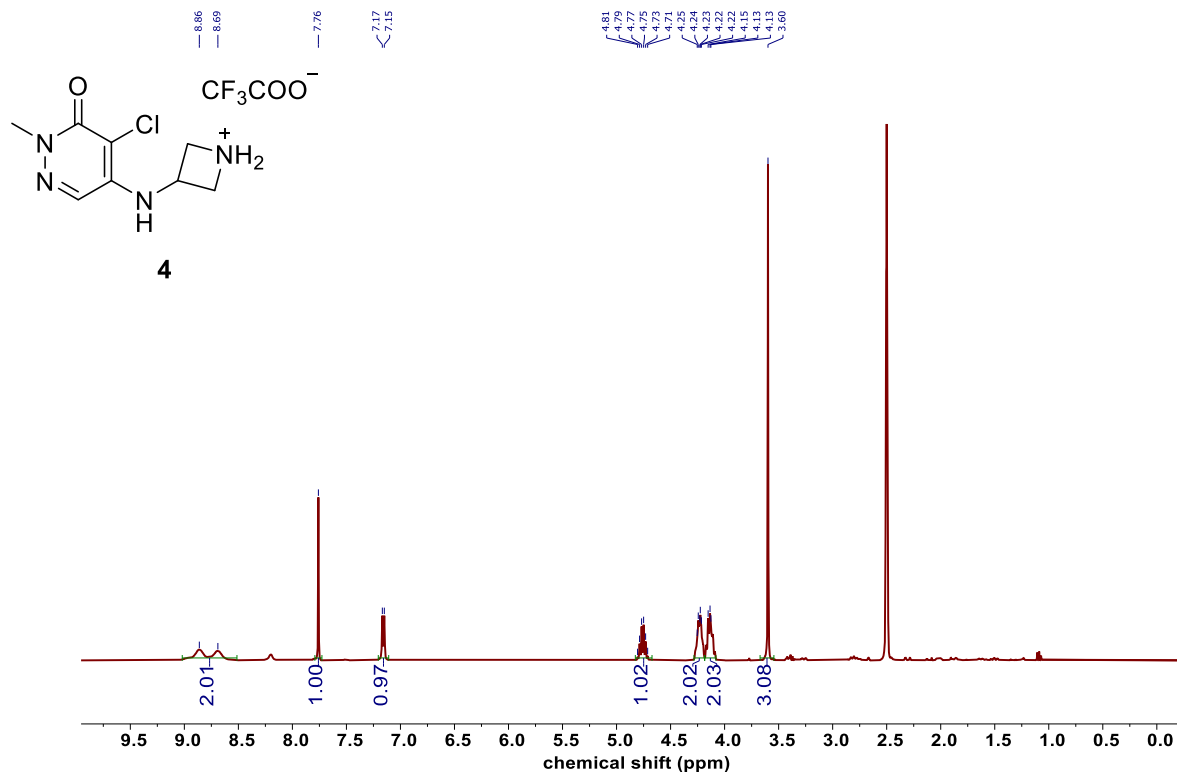
	19
PDB ID	7M2E
Data collection	
Resolution range	33.1 - 1.75 (1.81 - 1.75)
Wavelength (Å)	1.000
Space group	<i>P</i> 2 ₁
Unit cell (Å): <i>a</i> , <i>b</i> , <i>c</i>	27.01, 66.55, 39.62
(°): β	105.61
Total number of observed reflections	47148 (4142)
Unique reflections	12317 (1033)
Average mosaicity	0.56
Multiplicity	3.8 (2.9)
Completeness (%)	90.33 (75.90)
Mean <i>I</i> /σ(<i>I</i>)	9.6 (2.5)
Wilson B-factor	20.1
<i>R</i> _{merge} ^a	0.148 (0.391)
Structure refinement	
<i>R</i> _{work}	0.167 (0.199)
<i>R</i> _{free}	0.215 (0.253)
Molecules per asymmetric unit	1
Number of non-hydrogen atoms	1179
macromolecules	993
Ligand (CB02-092)	21
Solvent	165
Protein residues	121
RMS bond lengths (Å)	0.007
RMS bond angles (°)	0.81
Ramachandran favored (%)	100.0
Ramachandran allowed (%)	0.0
Ramachandran outliers (%)	0.0
Rotamer outliers (%)	0.92
Clashscore	0.51
Mean <i>B</i> values (Å²)	
Overall	23.4
macromolecules	22.0
Ligand (CB02-092)	26.4
Solvent	31.3

Parentheses numbers represent the highest-resolution shell.

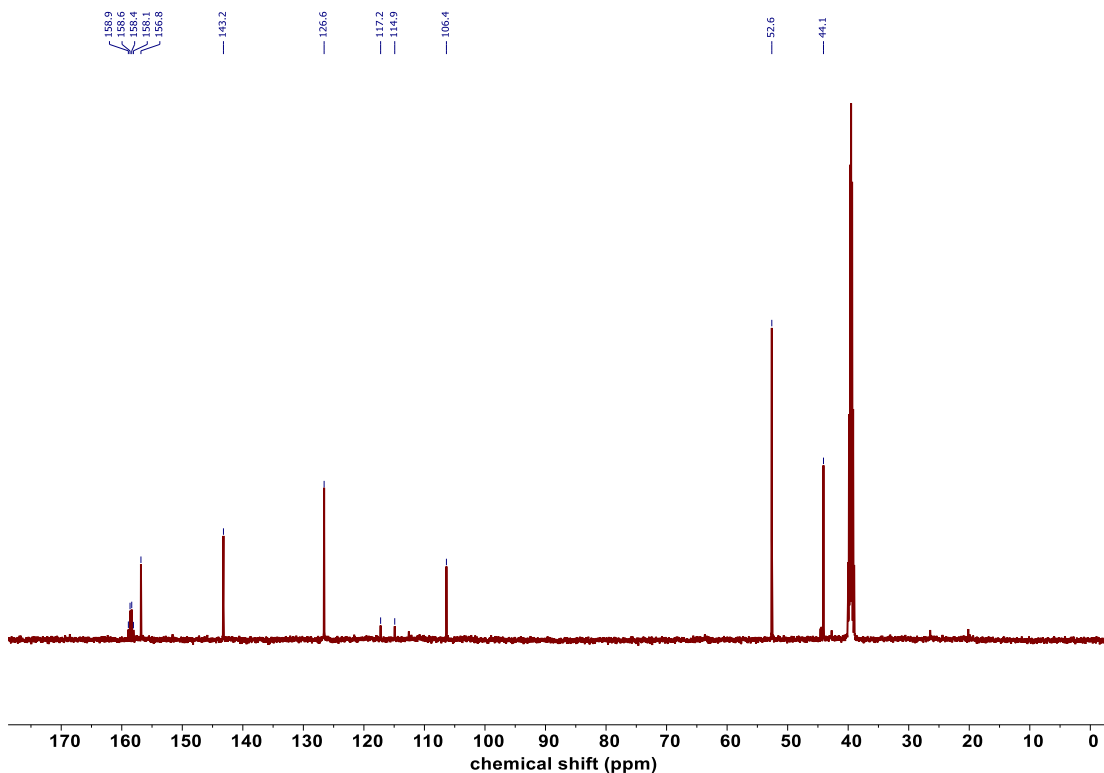
$$^a R_{\text{merge}} = \frac{\sum_{hkl} \sum_i |I_i(hkl) - I_{\text{av}}(hkl)|}{\sum_{hkl} \sum_i I_i(hkl)}.$$

¹H and ¹³C NMR spectra of small molecule analogues

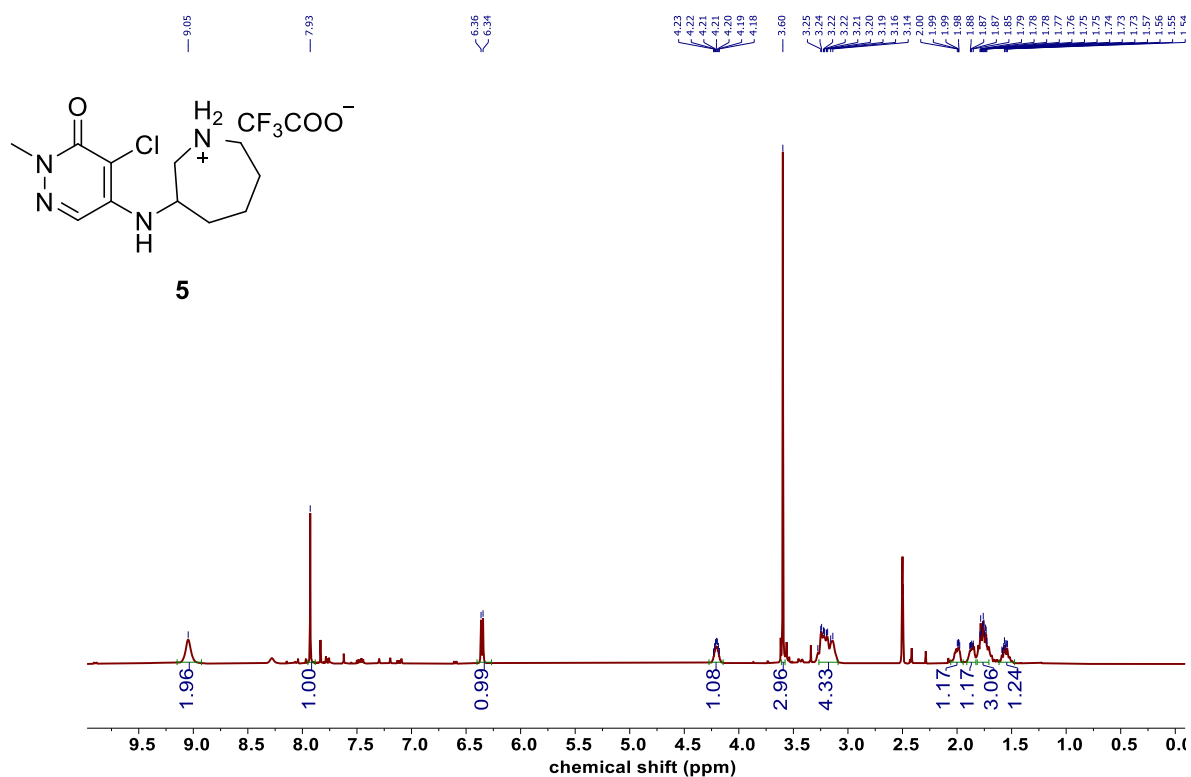
4, ¹H NMR (400 MHz, DMSO-d₆)



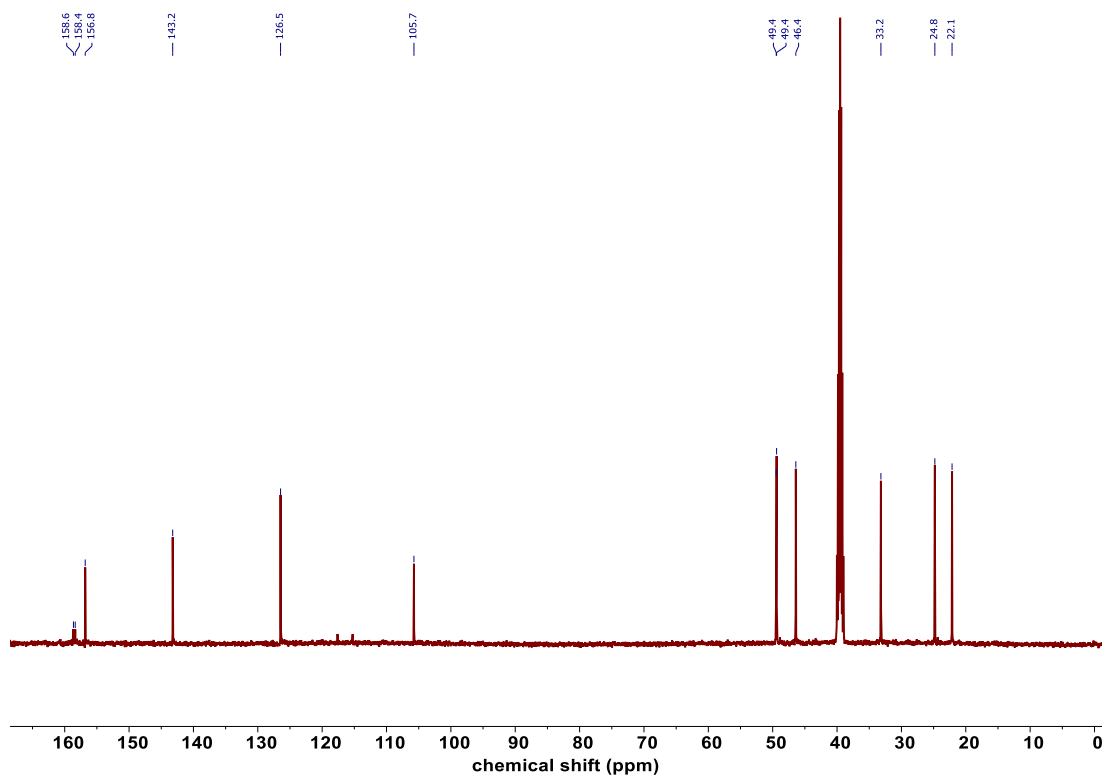
4, ¹³C NMR (126 MHz, DMSO-d₆)



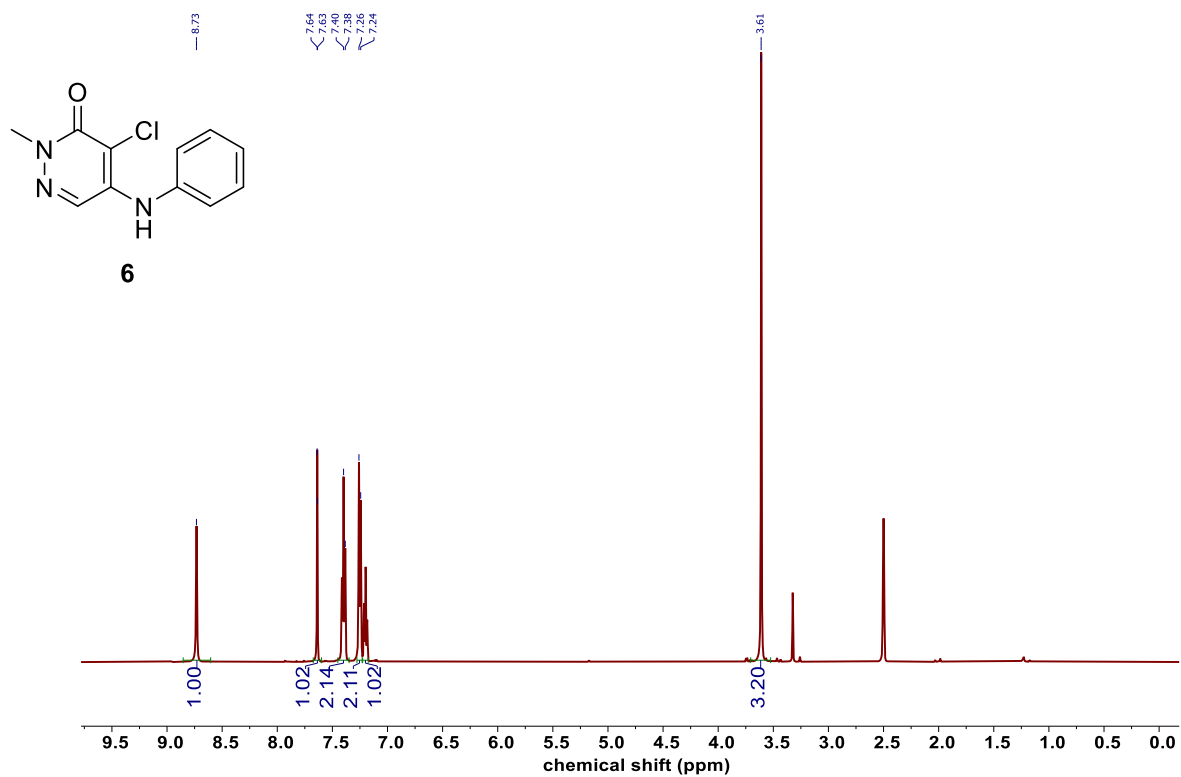
5, ¹H NMR (500 MHz, DMSO-d₆)



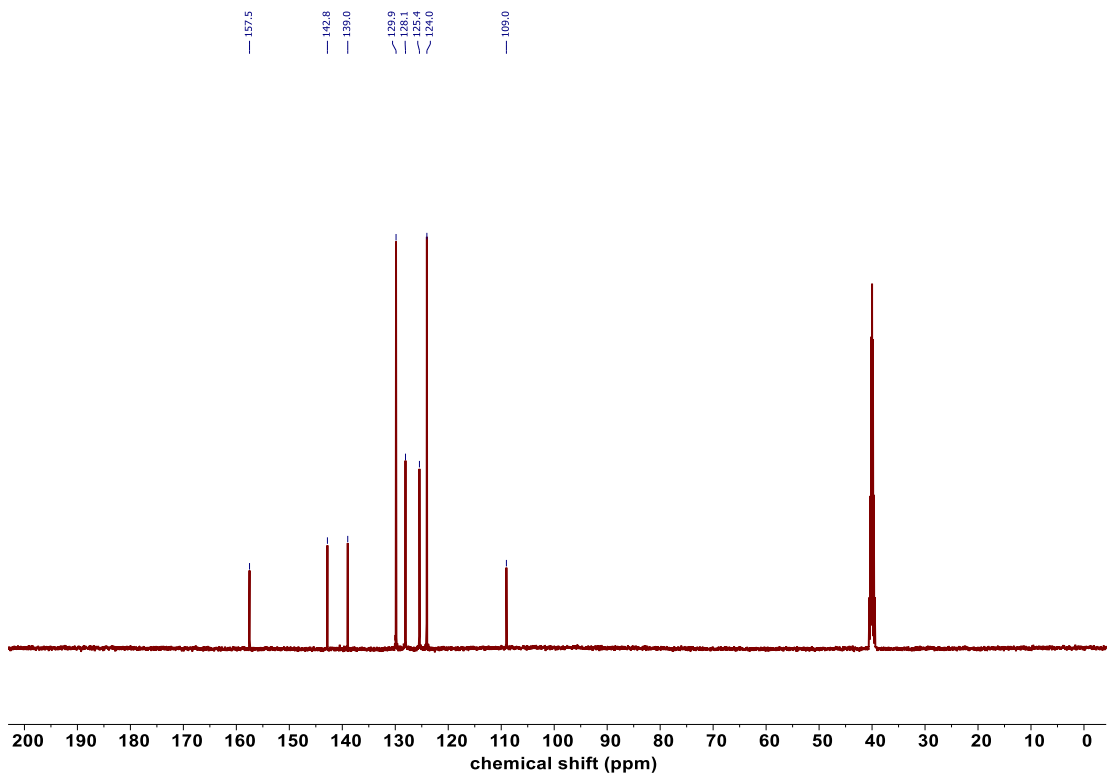
5, ¹³C NMR (126 MHz, DMSO-d₆)



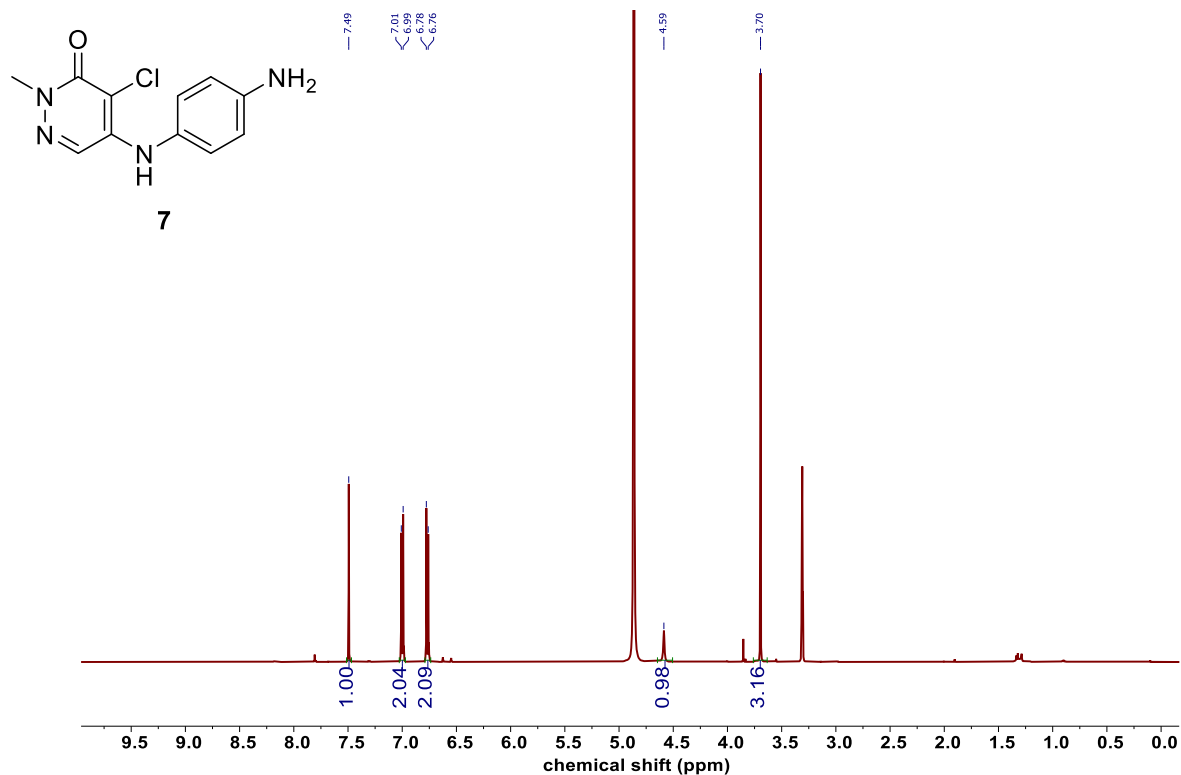
6, ¹H NMR (500 MHz, DMSO-d₆)



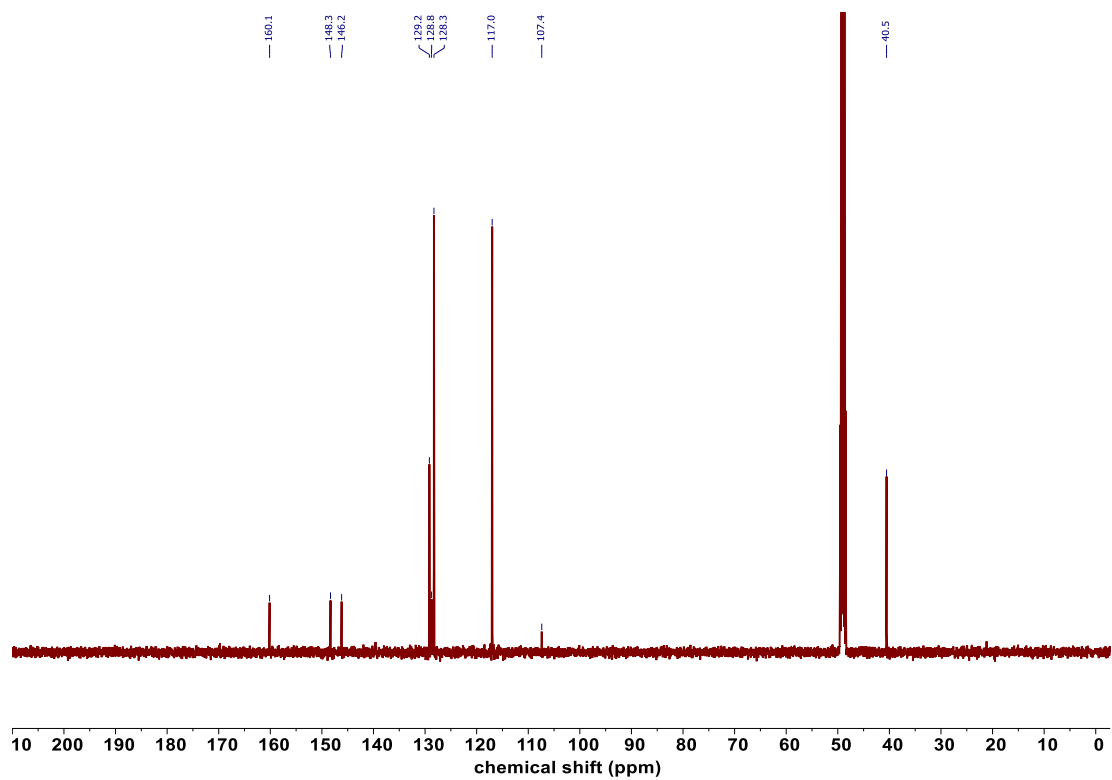
6, ¹³C NMR (126 MHz, DMSO-d₆)



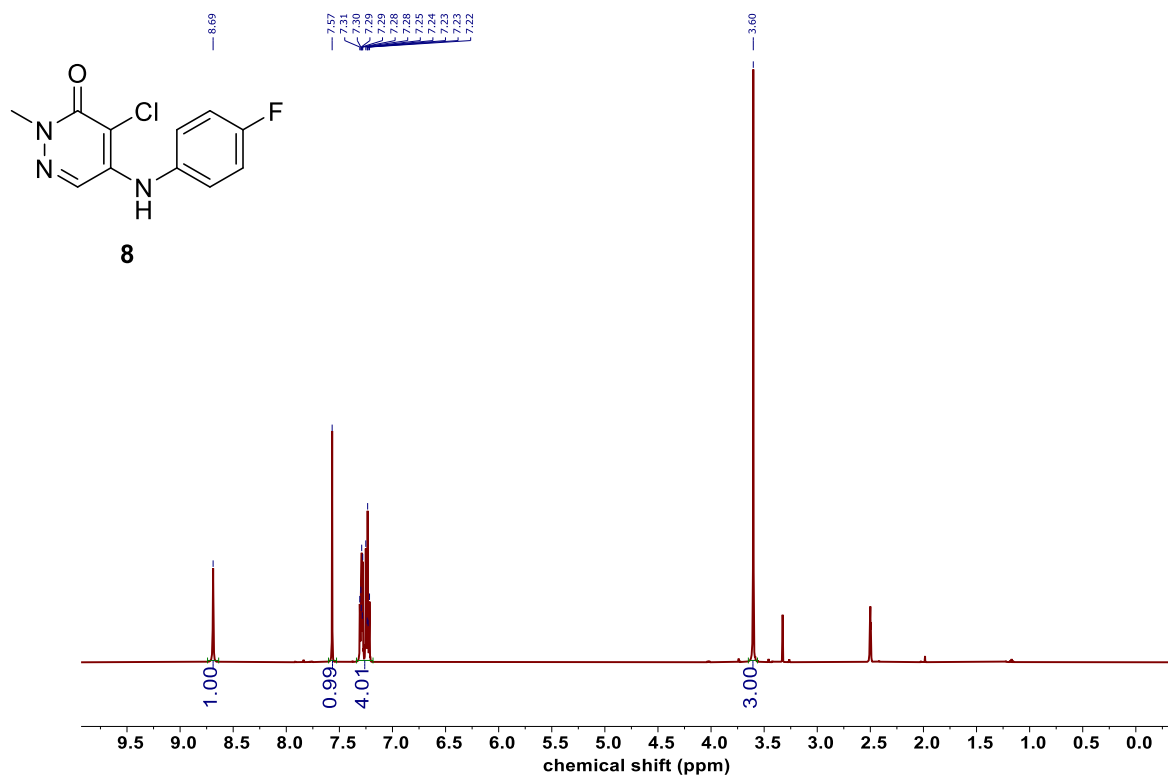
7, ¹H NMR (500 MHz, Methanol-d₄)



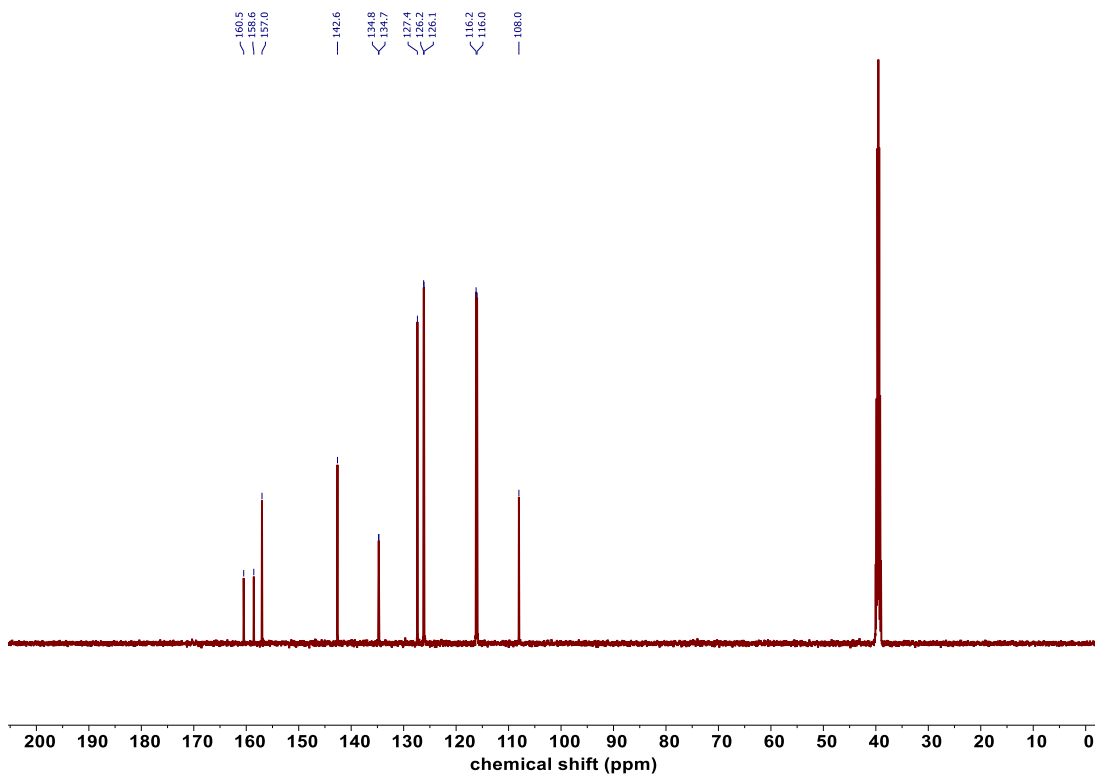
7, ¹³C NMR (126 MHz, Methanol-d₄)



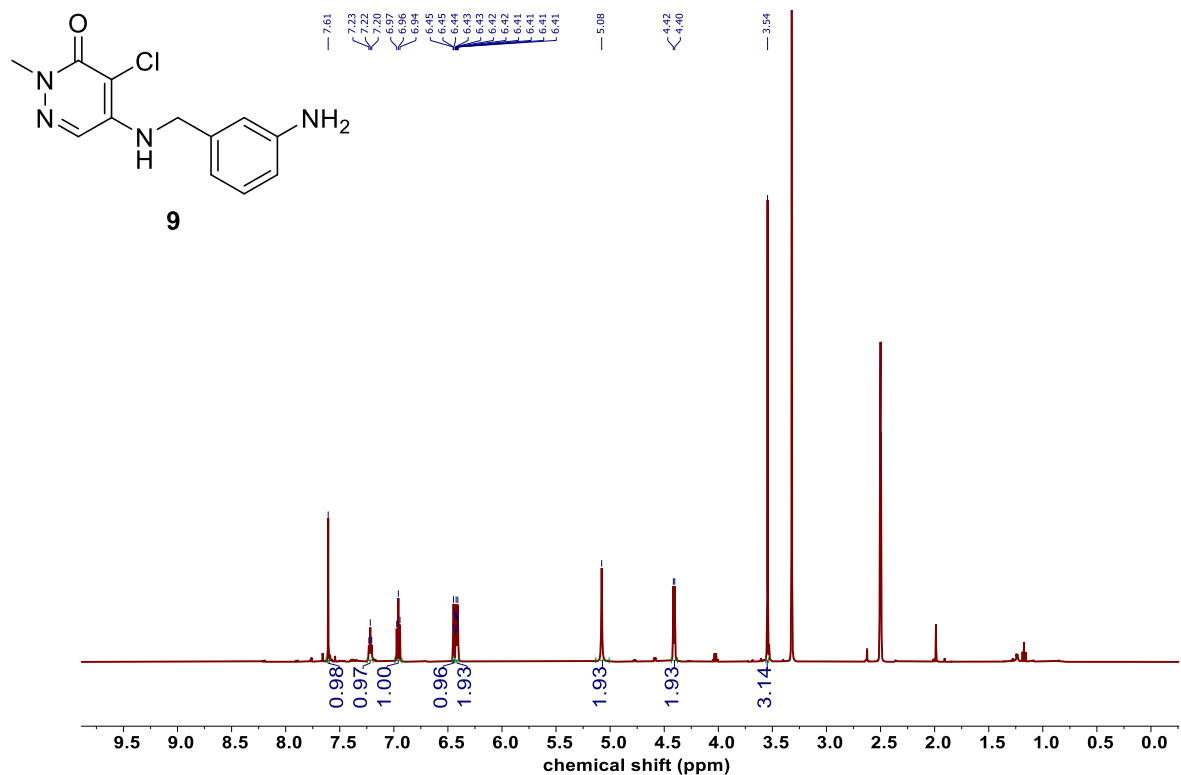
8, ^1H NMR (500 MHz, $\text{DMSO-}d_6$)



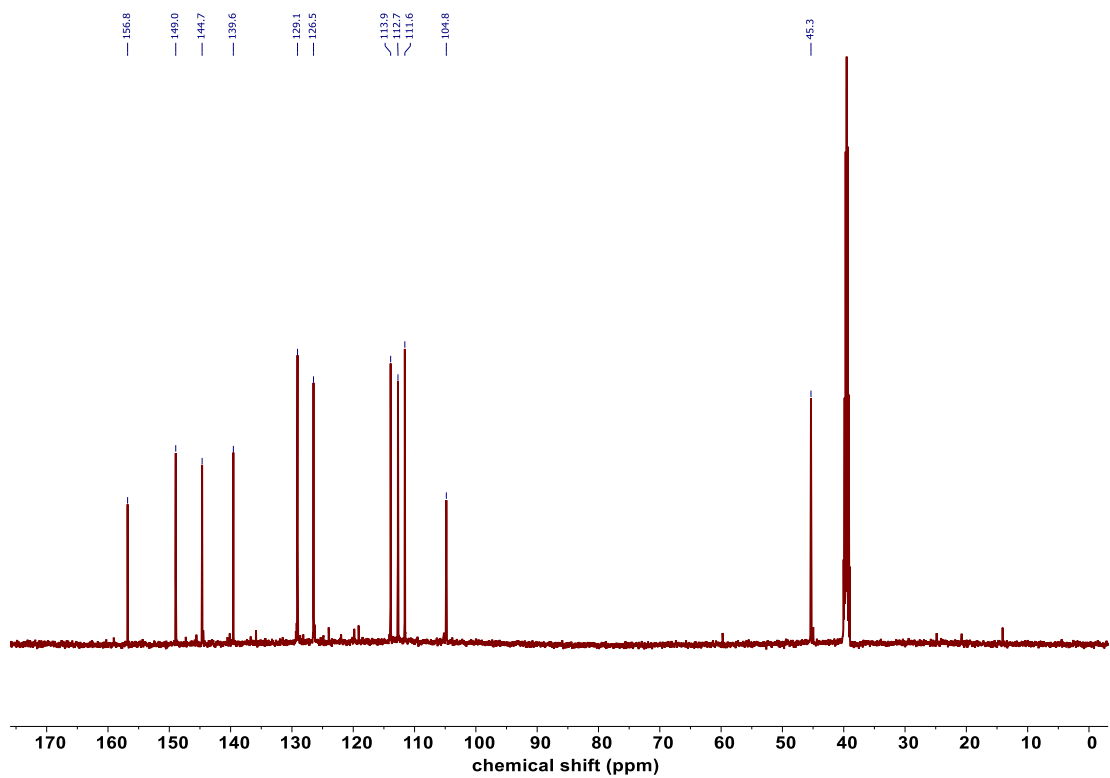
8, ^{13}C NMR (126 MHz, $\text{DMSO-}d_6$)



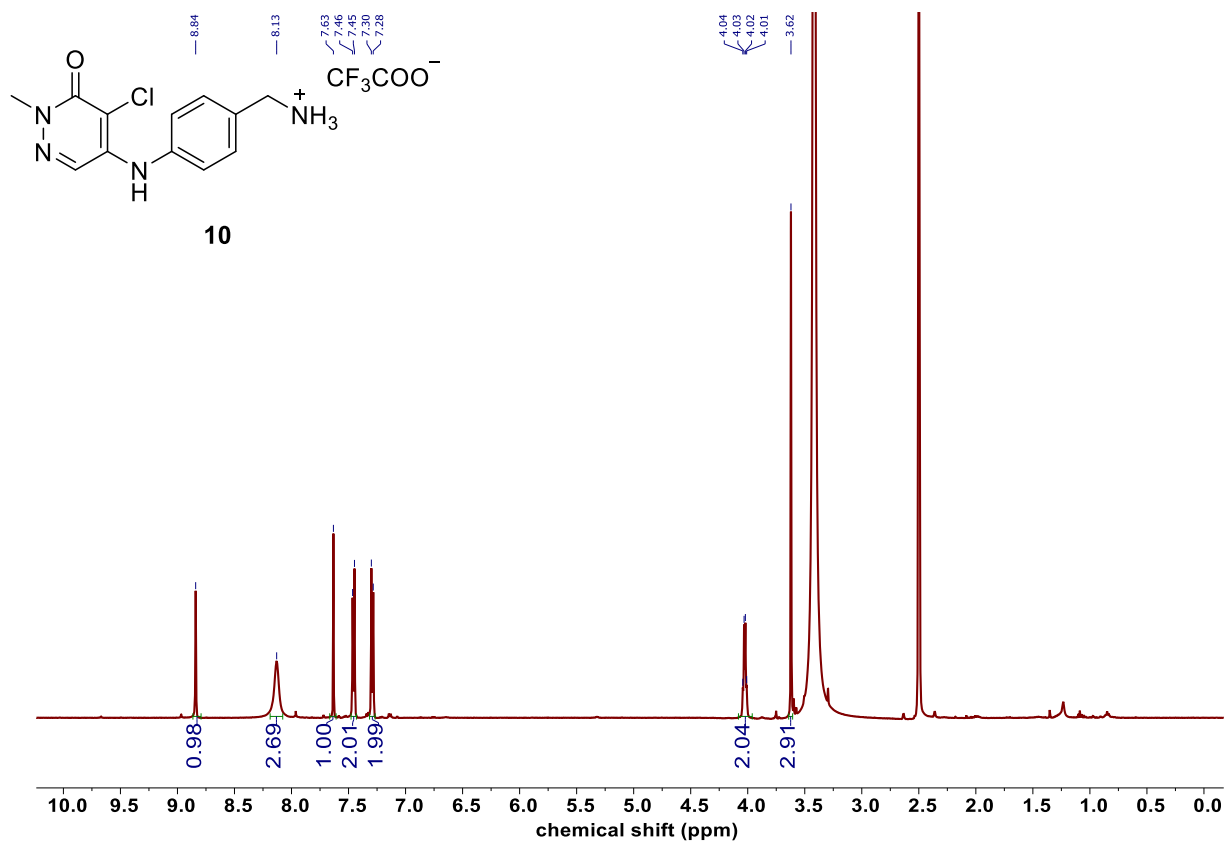
9, ¹H NMR (500 MHz, DMSO-d₆)



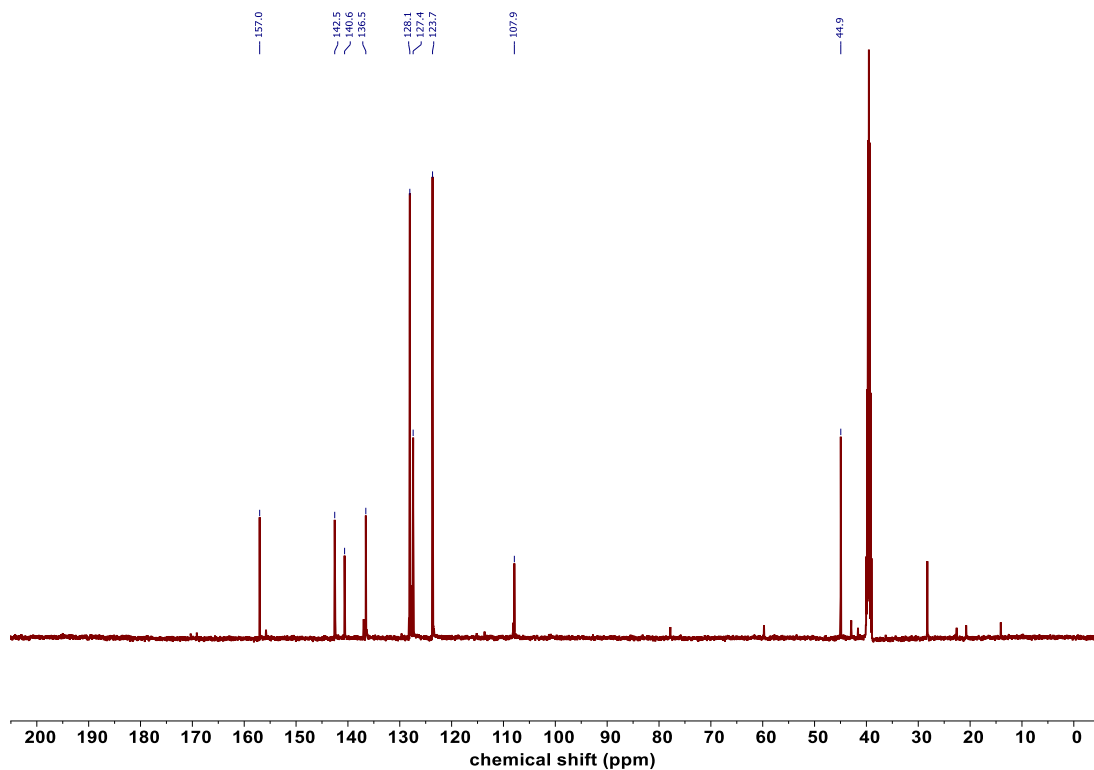
9, ¹³C NMR (126 MHz, DMSO-d₆)



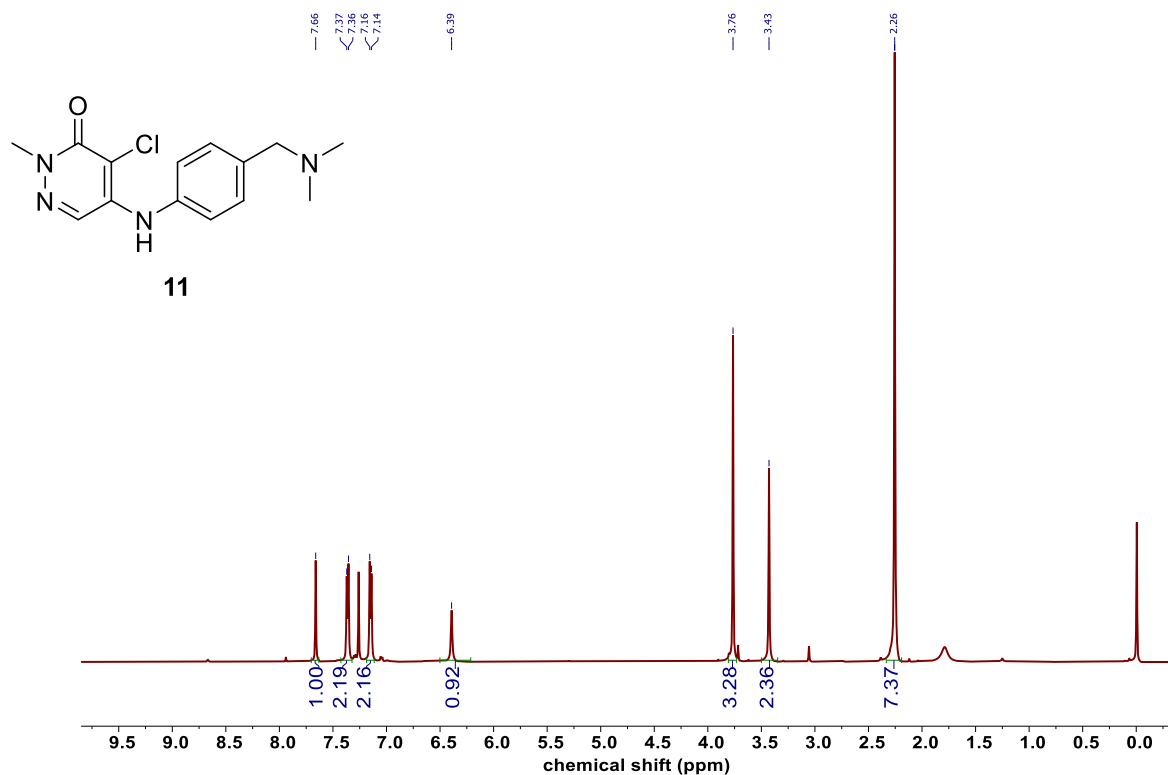
10, ^1H NMR (500 MHz, $\text{DMSO-}d_6$)



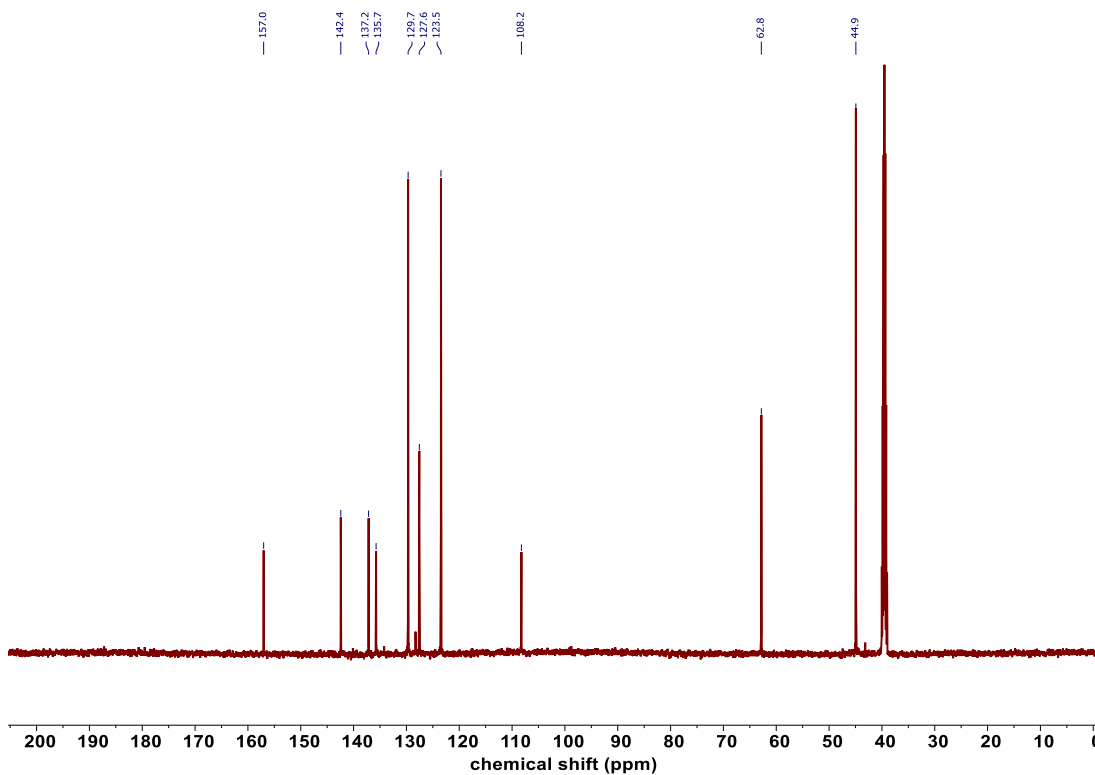
10, ^{13}C NMR (126 MHz, $\text{DMSO-}d_6$)



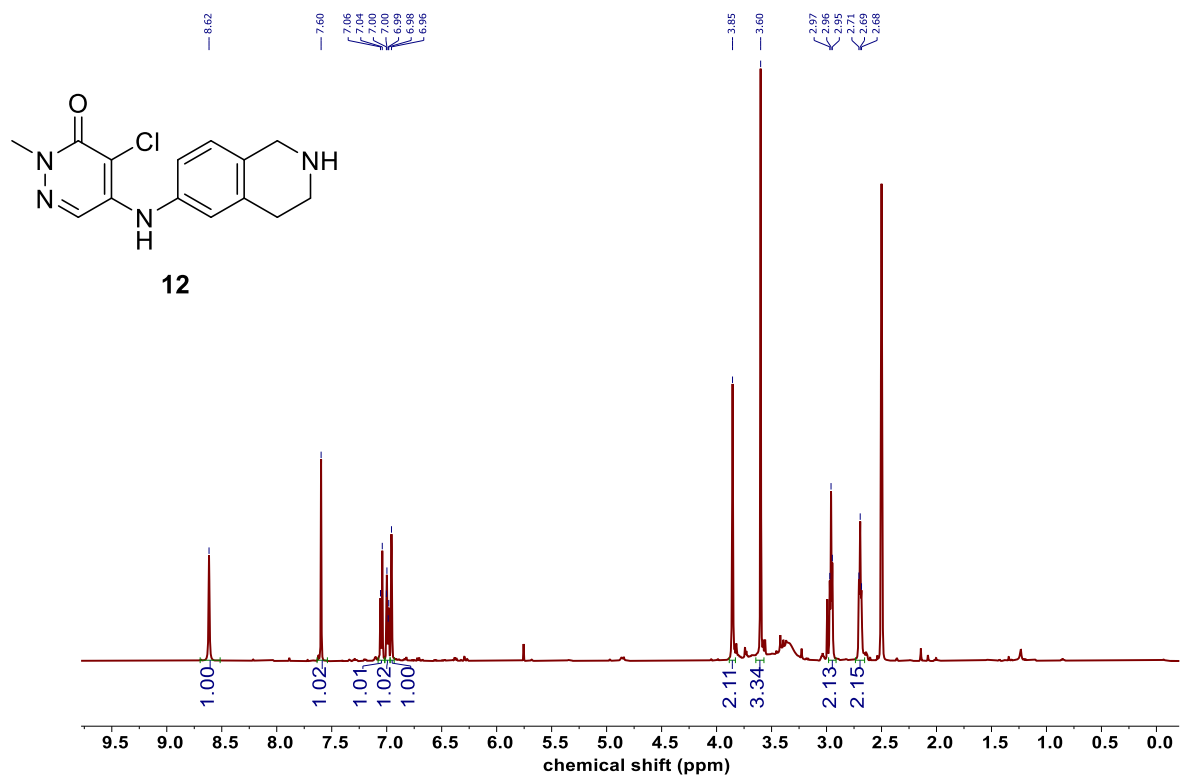
11, ^1H NMR (500 MHz, Chloroform-*d*)



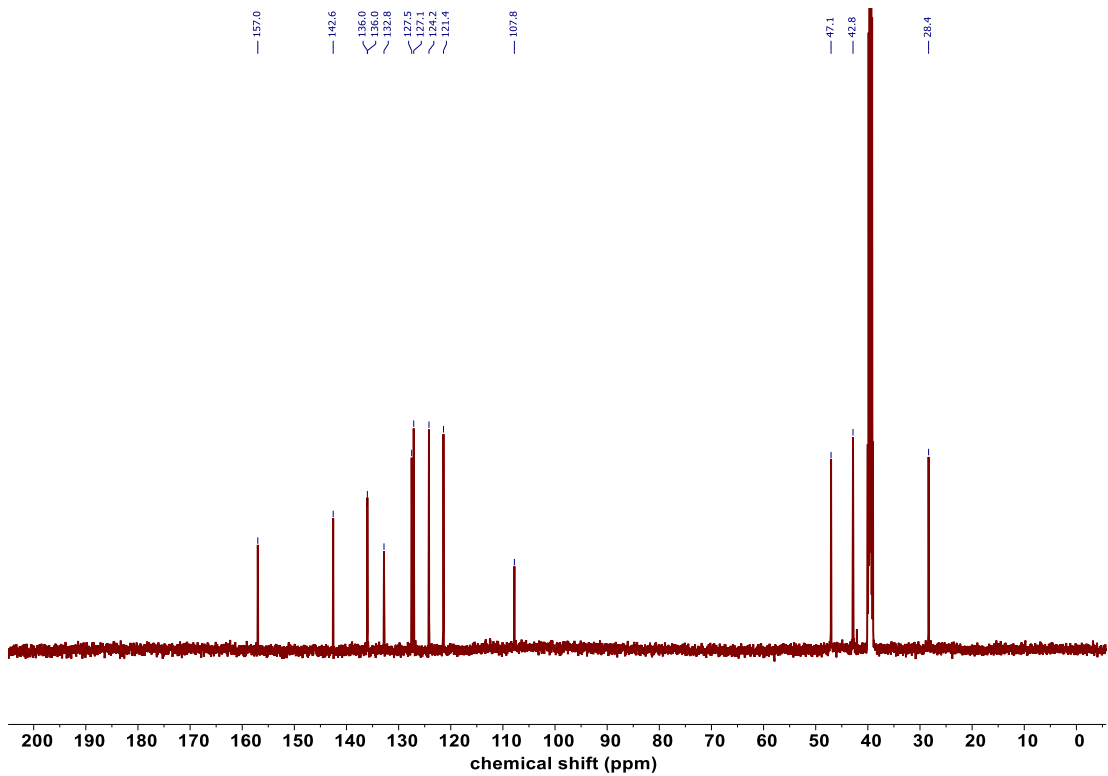
11, ^{13}C NMR (126 MHz, DMSO-*d*₆)



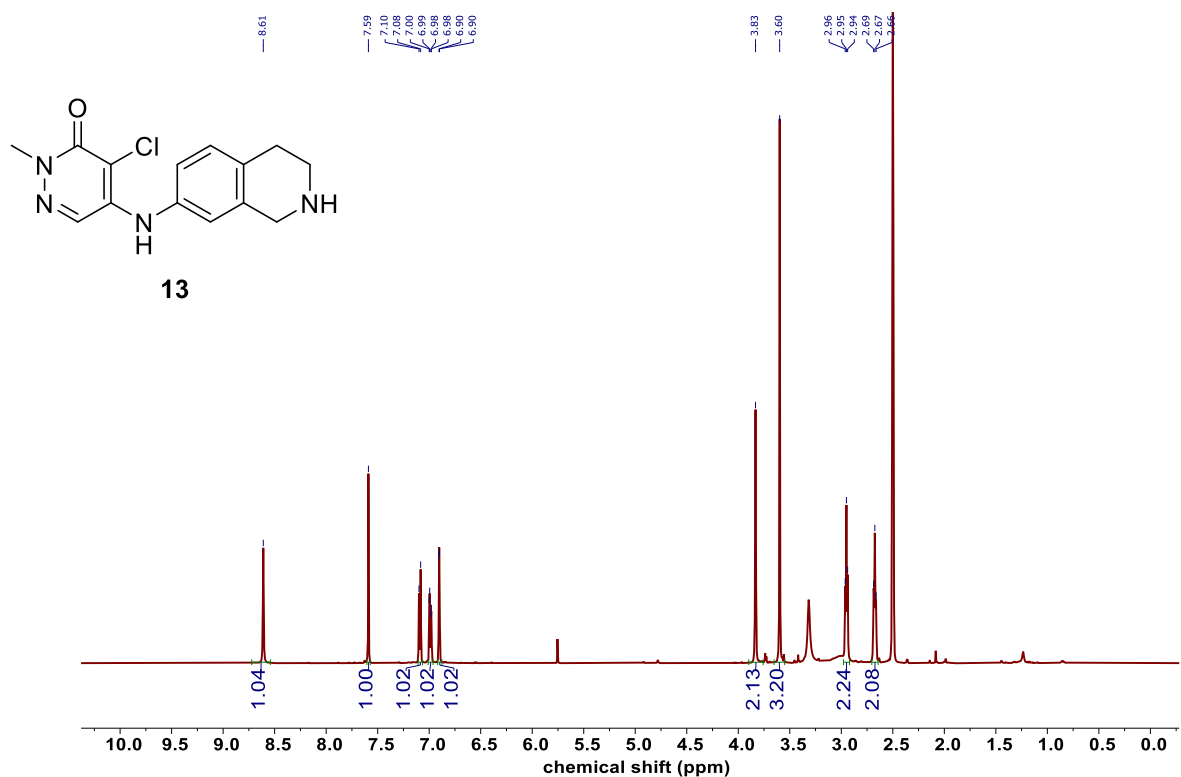
12, ^1H NMR (500 MHz, $\text{DMSO-}d_6$)



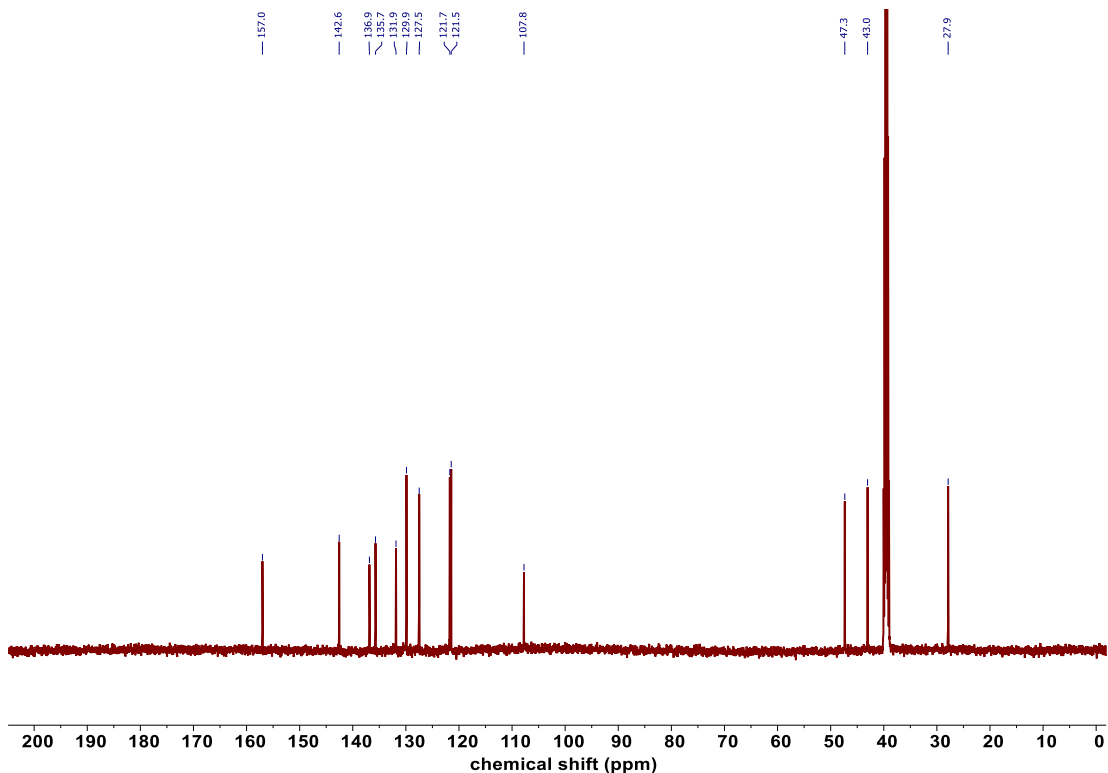
12, ^{13}C NMR (126 MHz, $\text{DMSO-}d_6$)



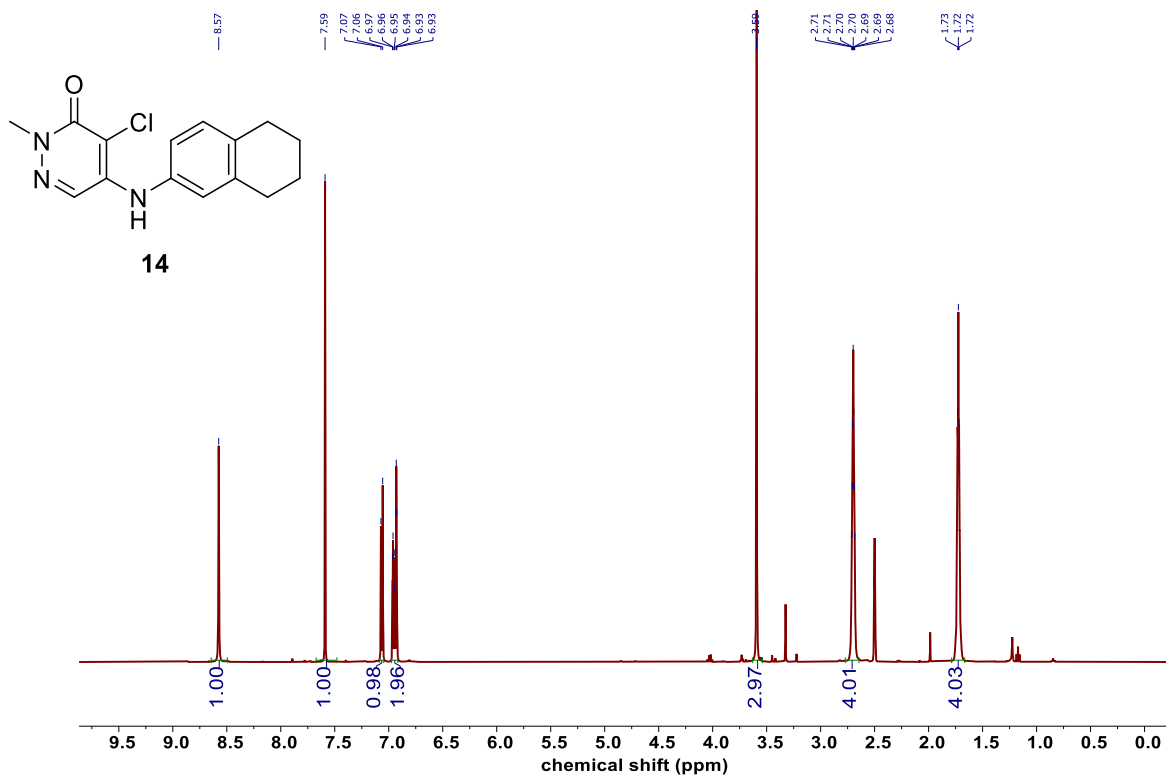
13, ^1H NMR (500 MHz, $\text{DMSO}-d_6$)



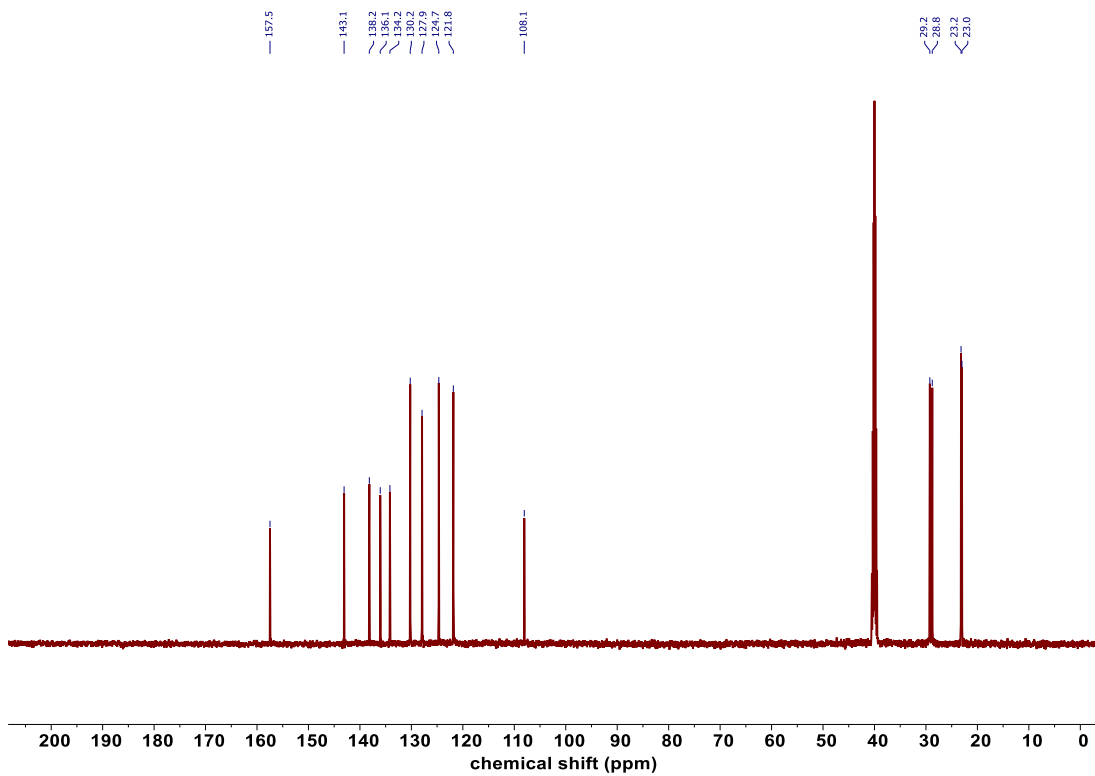
13, ^{13}C NMR (126 MHz, $\text{DMSO}-d_6$)



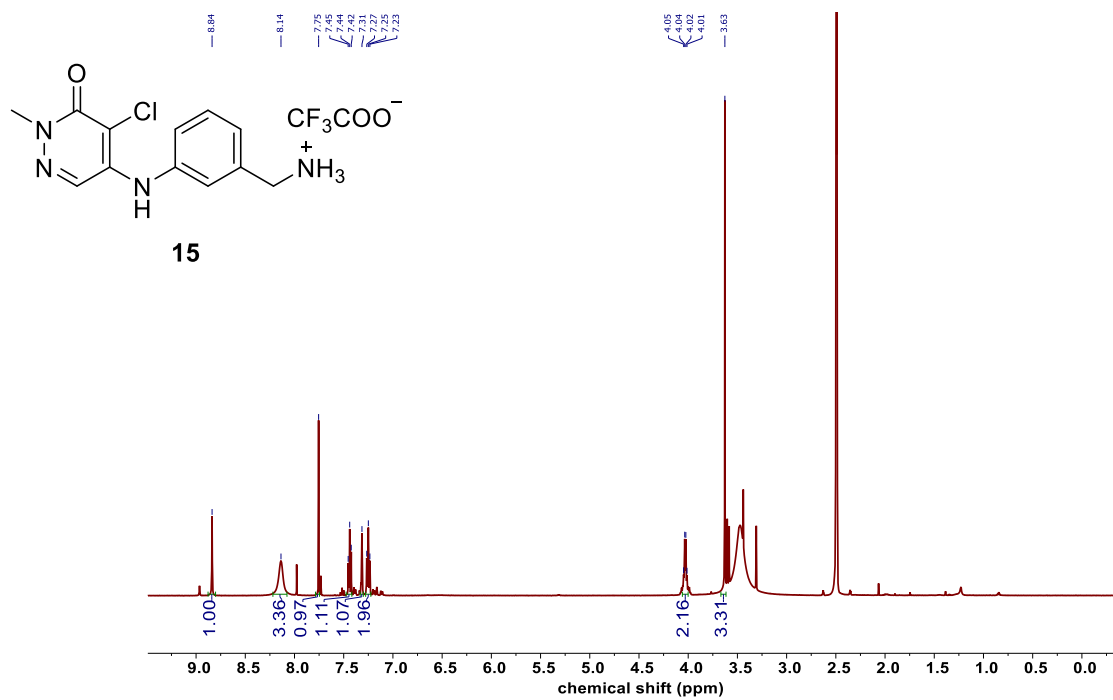
14, ^1H NMR (500 MHz, $\text{DMSO-}d_6$)



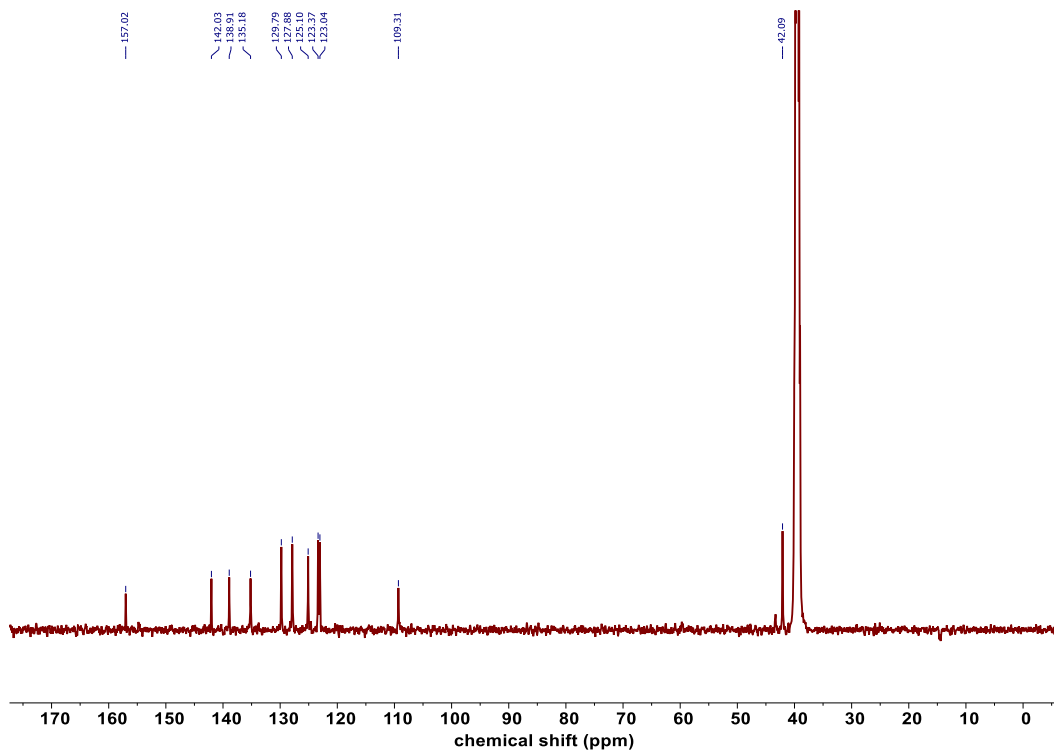
14, ^{13}C NMR (126 MHz, $\text{DMSO-}d_6$)



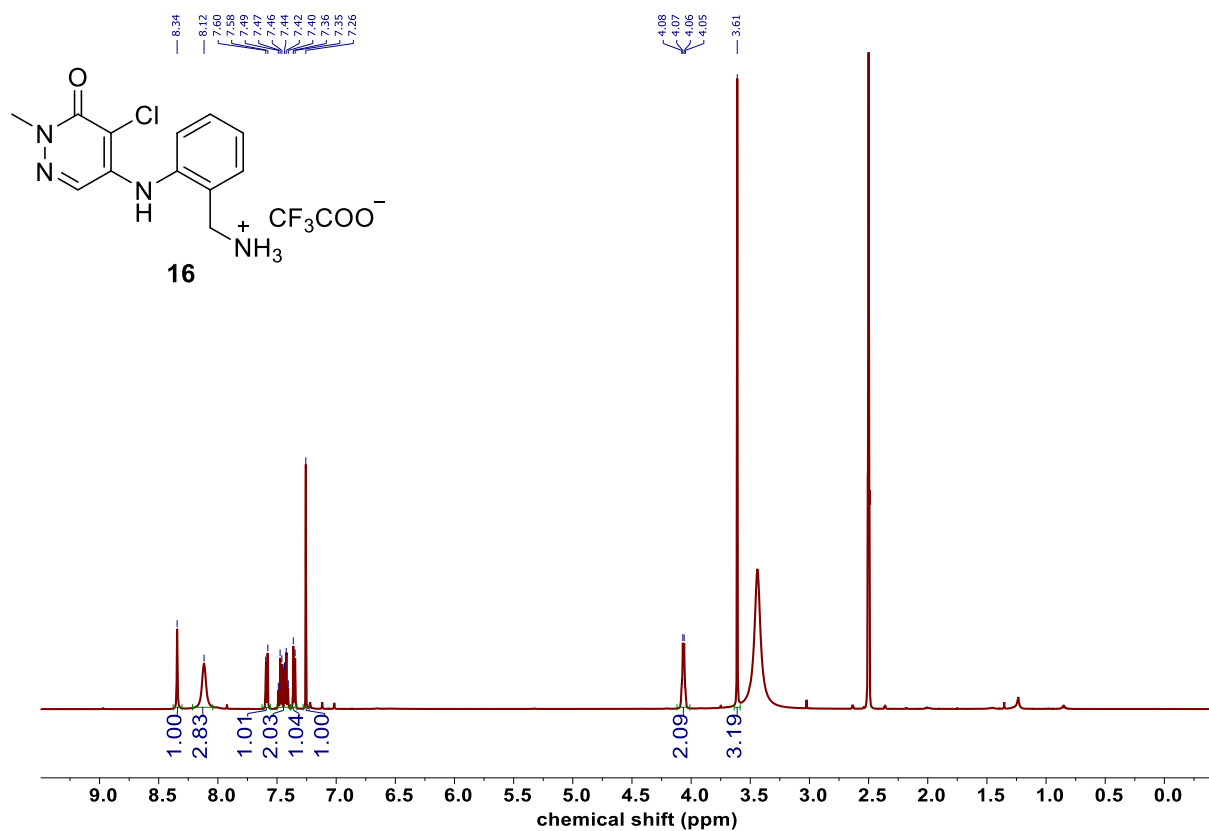
15, ¹H NMR (500 MHz, DMSO-*d*₆)



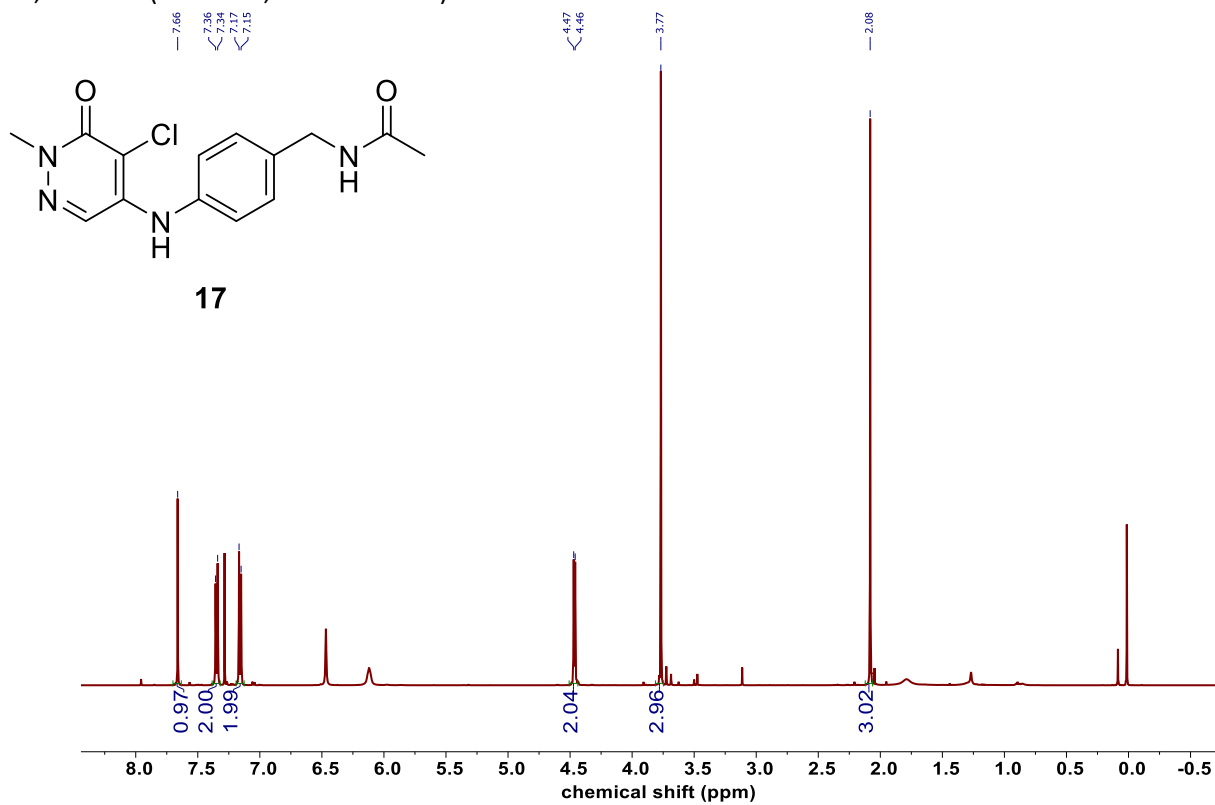
15, ¹³C NMR (126 MHz, DMSO-*d*₆)



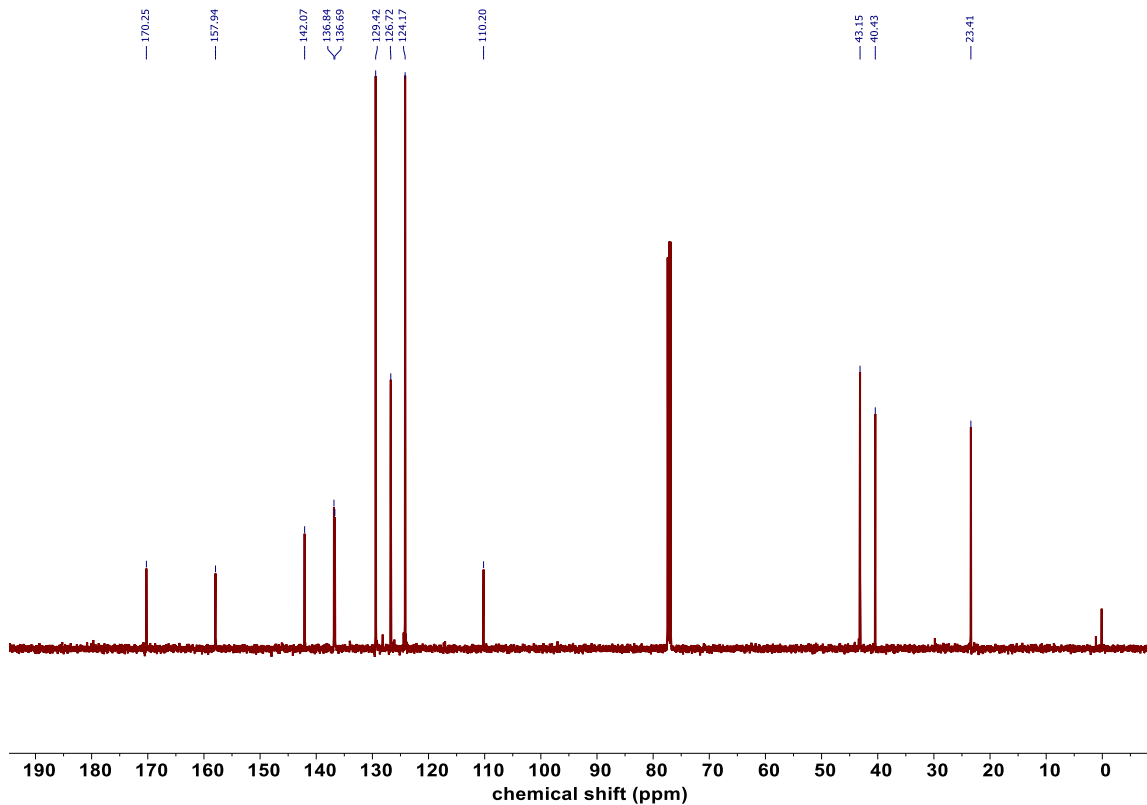
16, ¹H NMR (500 MHz, DMSO-d₆)



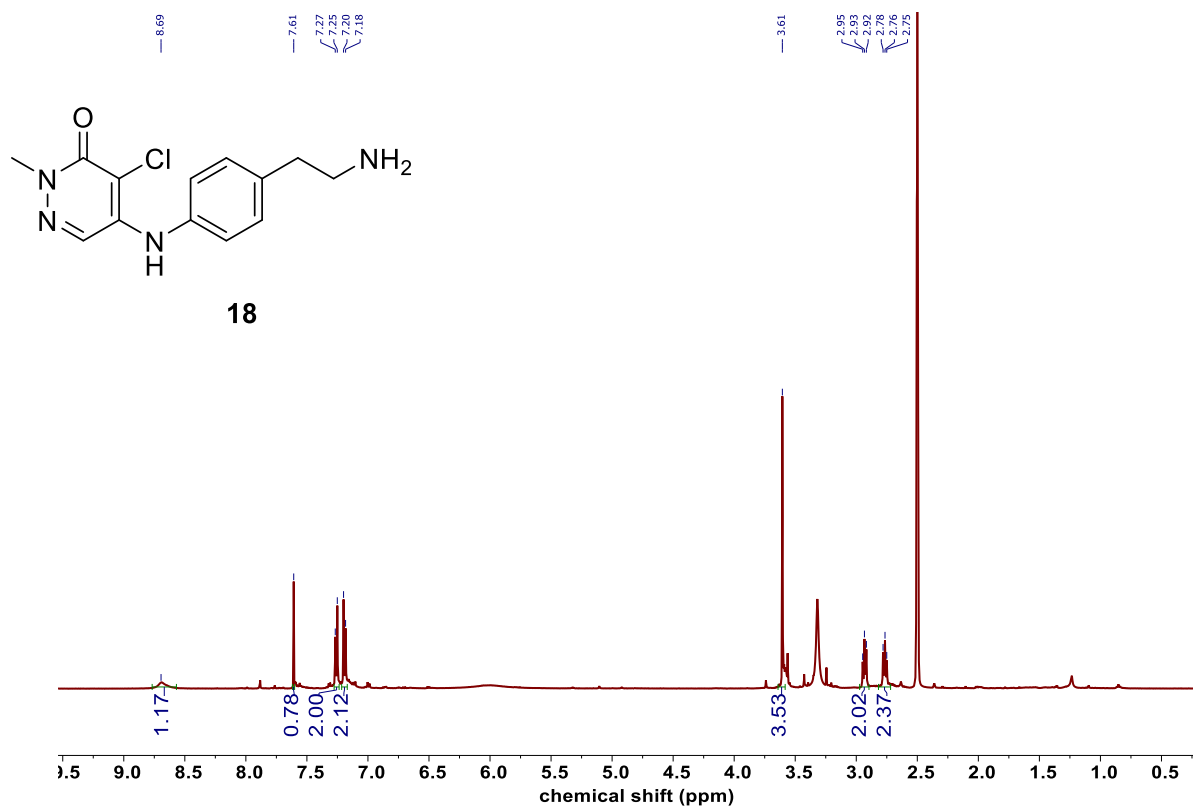
17, ¹H NMR (500 MHz, Chloroform-*d*)



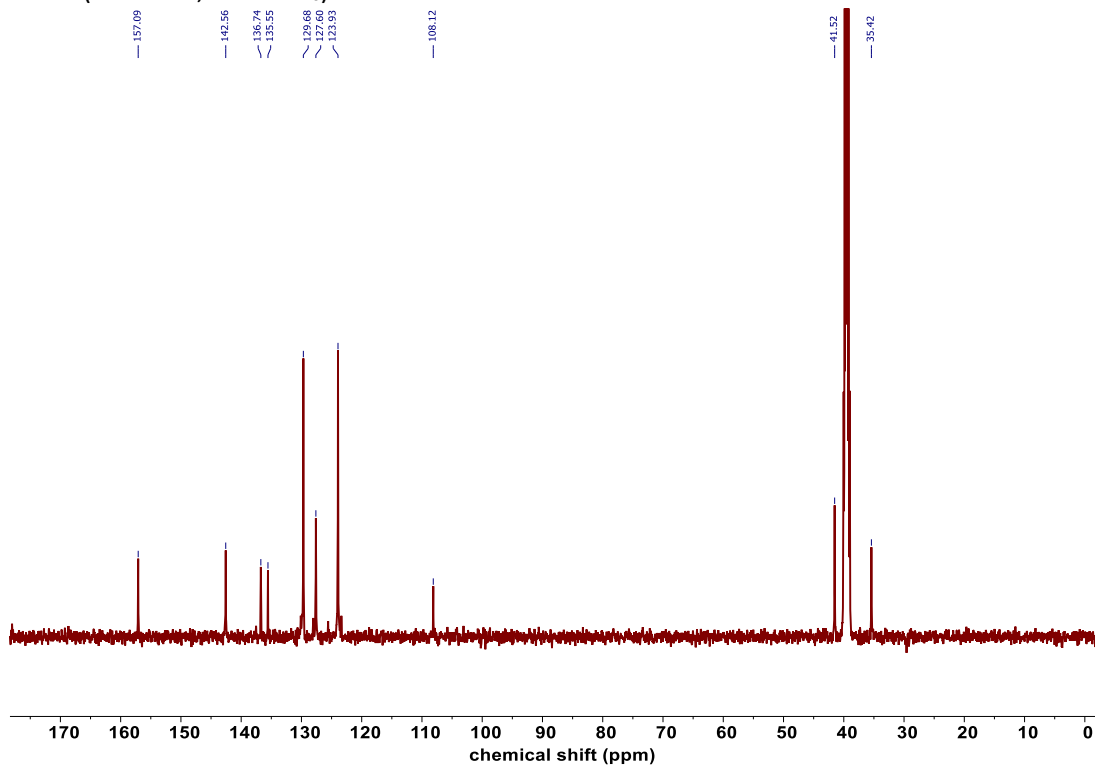
17, ¹³C NMR (126 MHz, Chloroform-*d*)



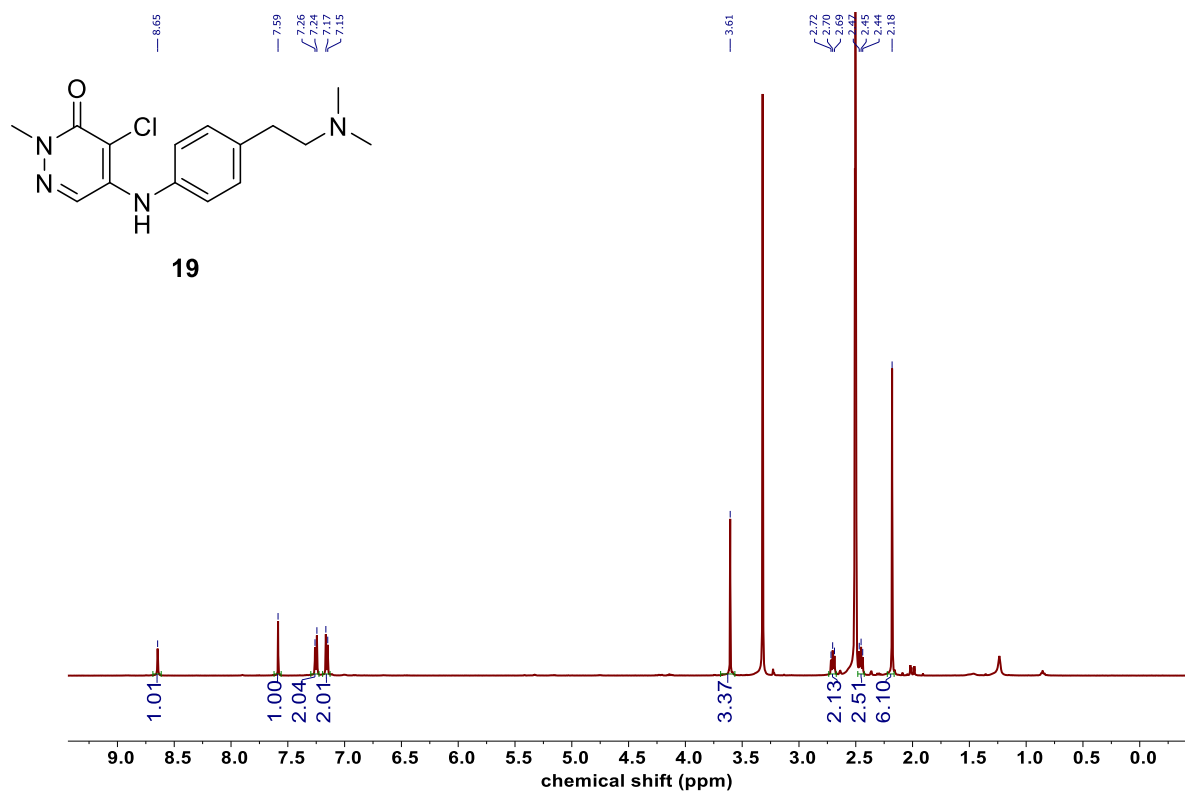
18, ^1H NMR (500 MHz, $\text{DMSO-}d_6$)



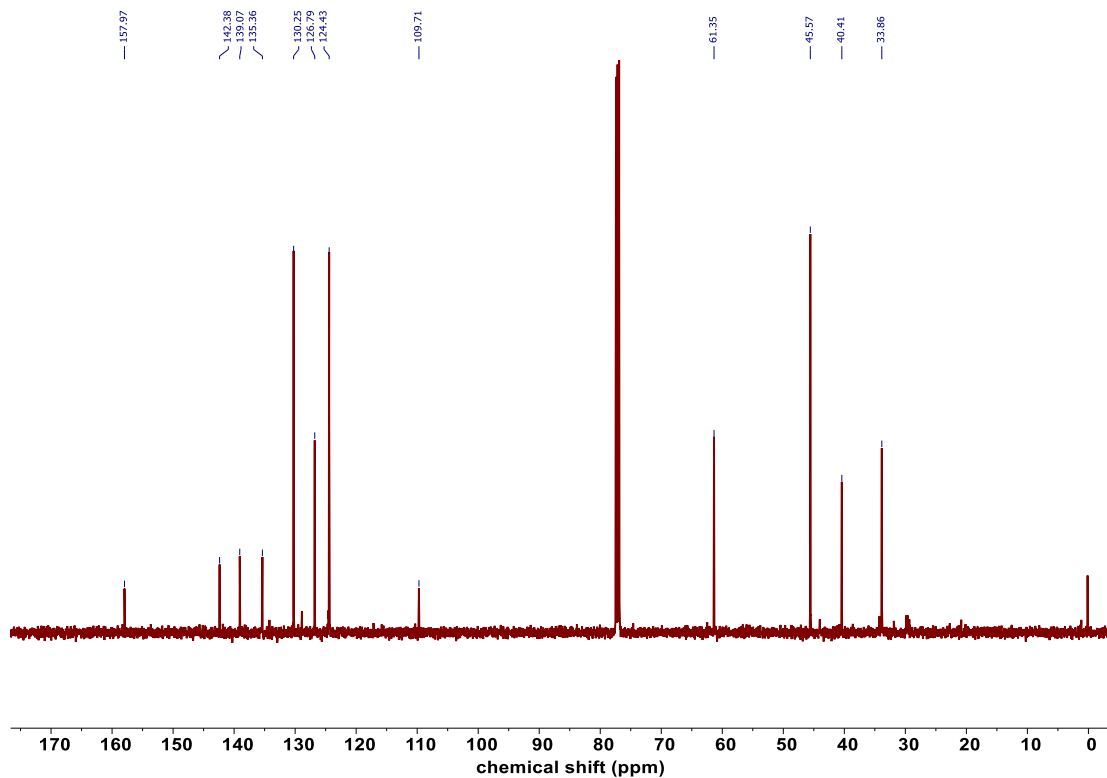
18, ^{13}C NMR (126 MHz, $\text{DMSO-}d_6$)



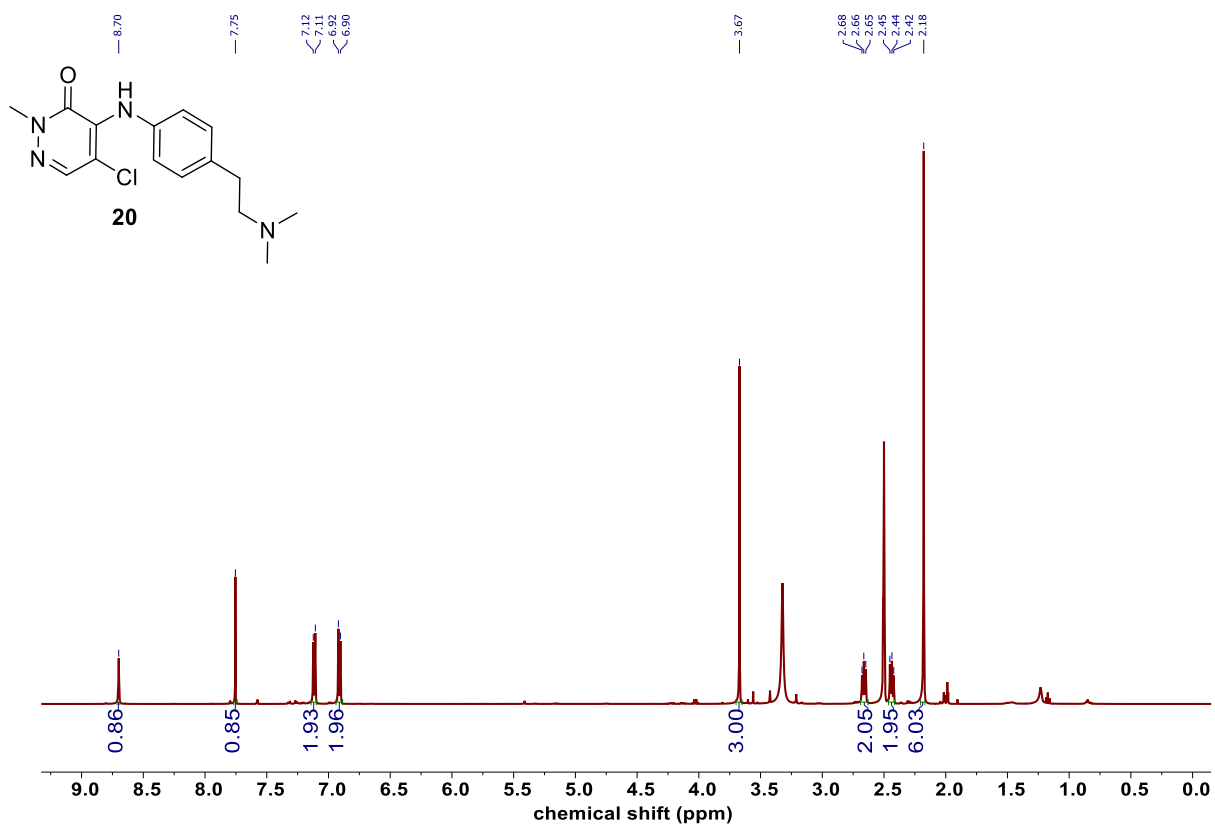
19, ^1H NMR (500 MHz, $\text{DMSO-}d_6$)



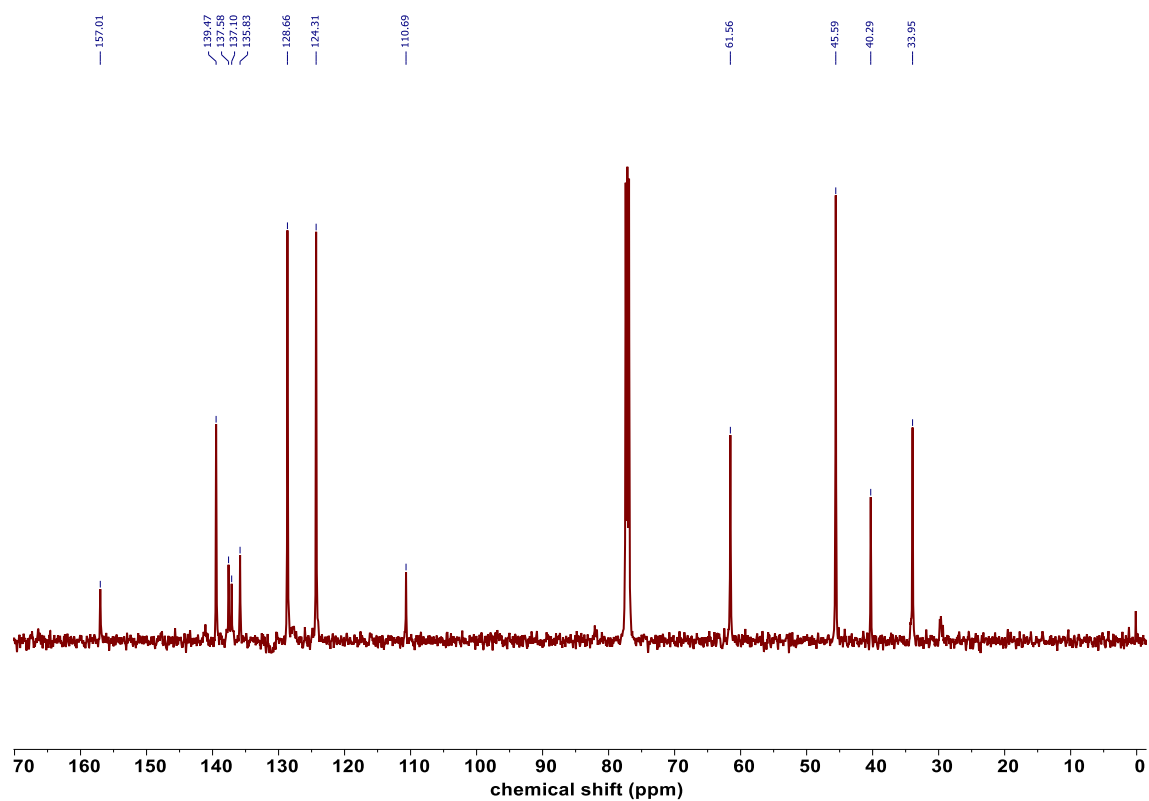
19, ^{13}C NMR (126 MHz, $\text{Chloroform-}d$)



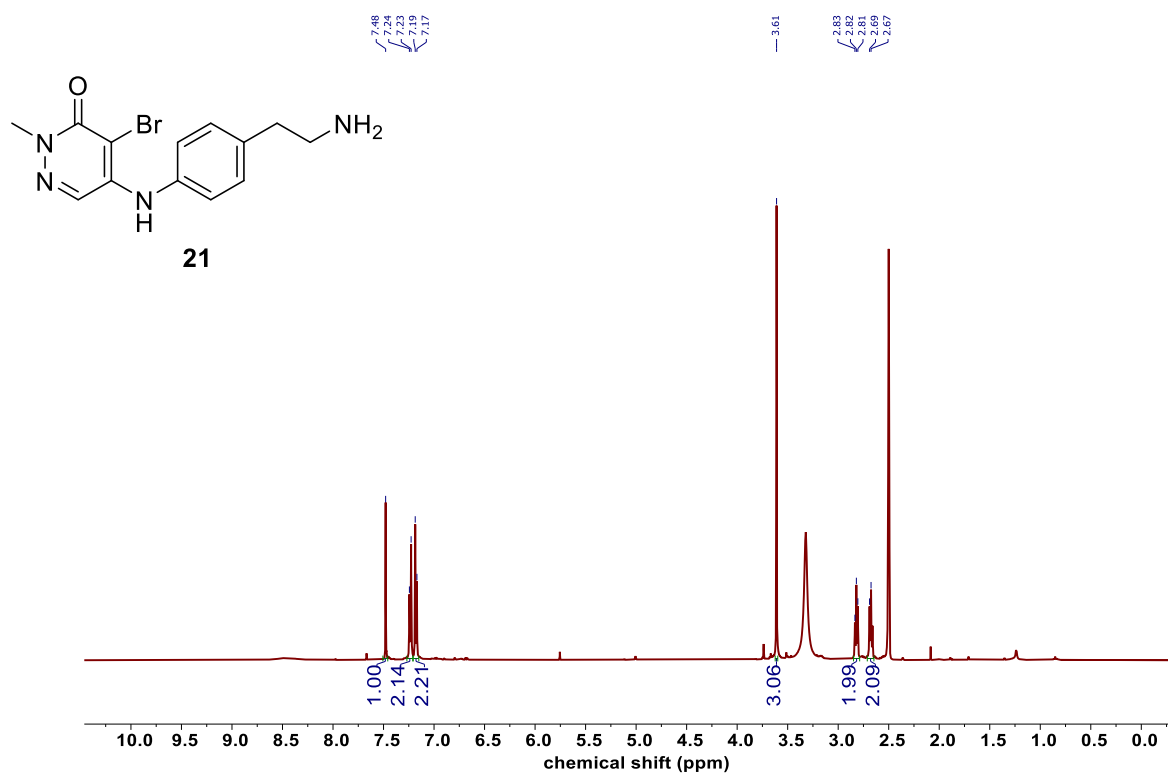
20, ^1H NMR (500 MHz, $\text{DMSO-}d_6$)



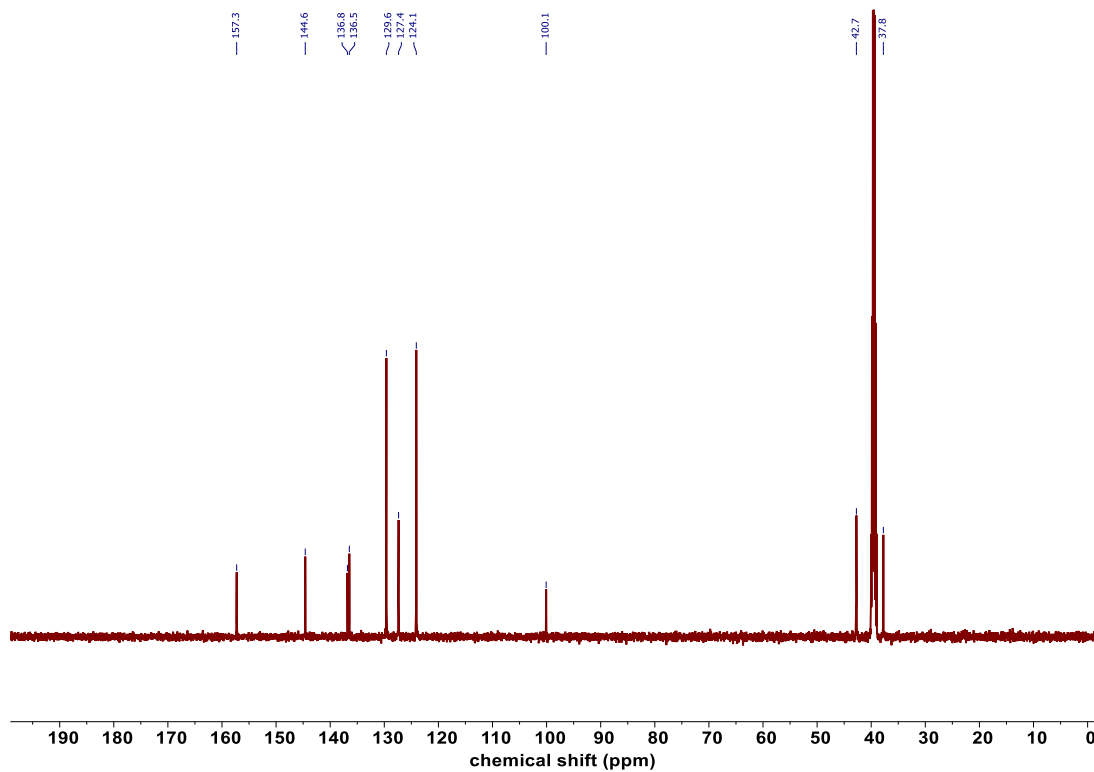
20, ^{13}C NMR (126 MHz, $\text{Chloroform-}d$)



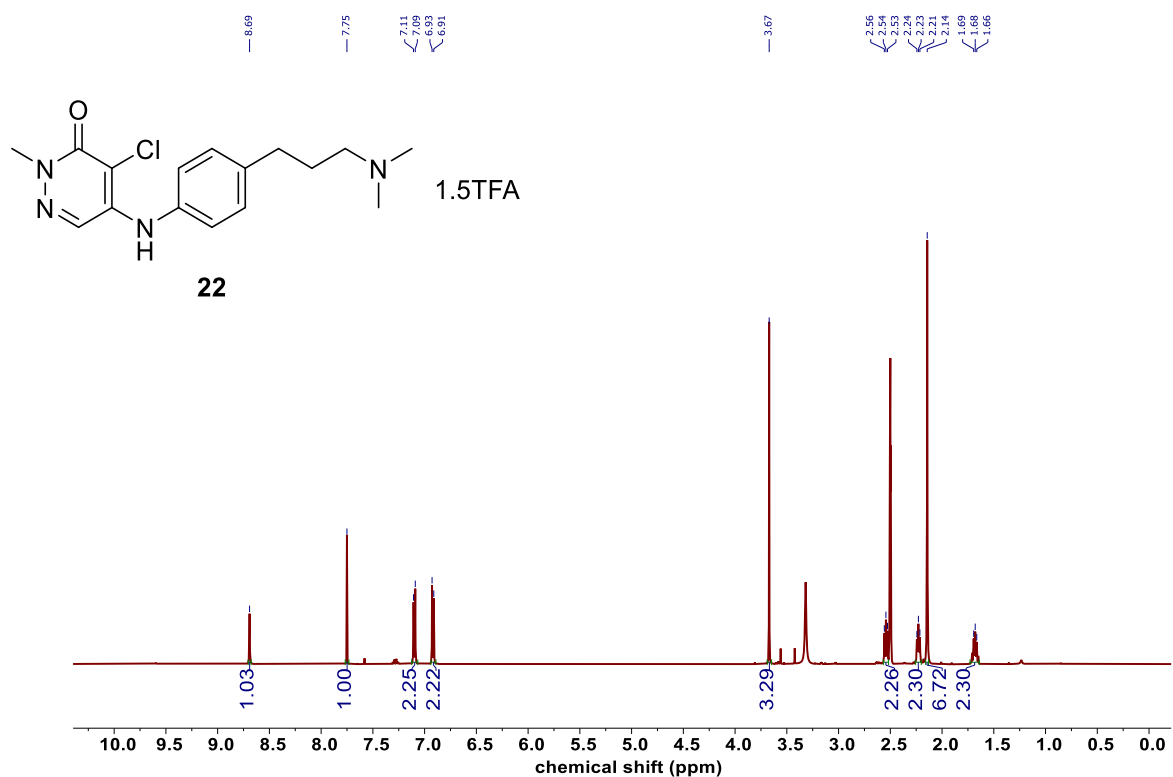
21, ^1H NMR (500 MHz, $\text{DMSO-}d_6$)



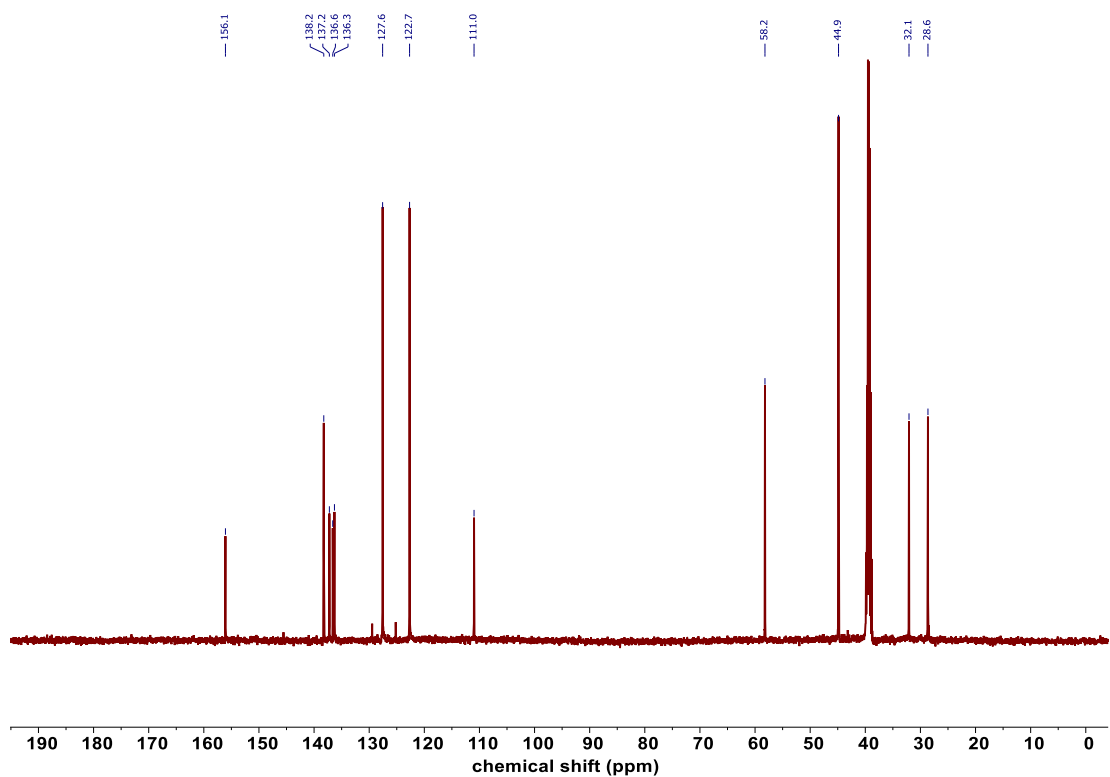
21, ^{13}C NMR (126 MHz, $\text{DMSO-}d_6$)



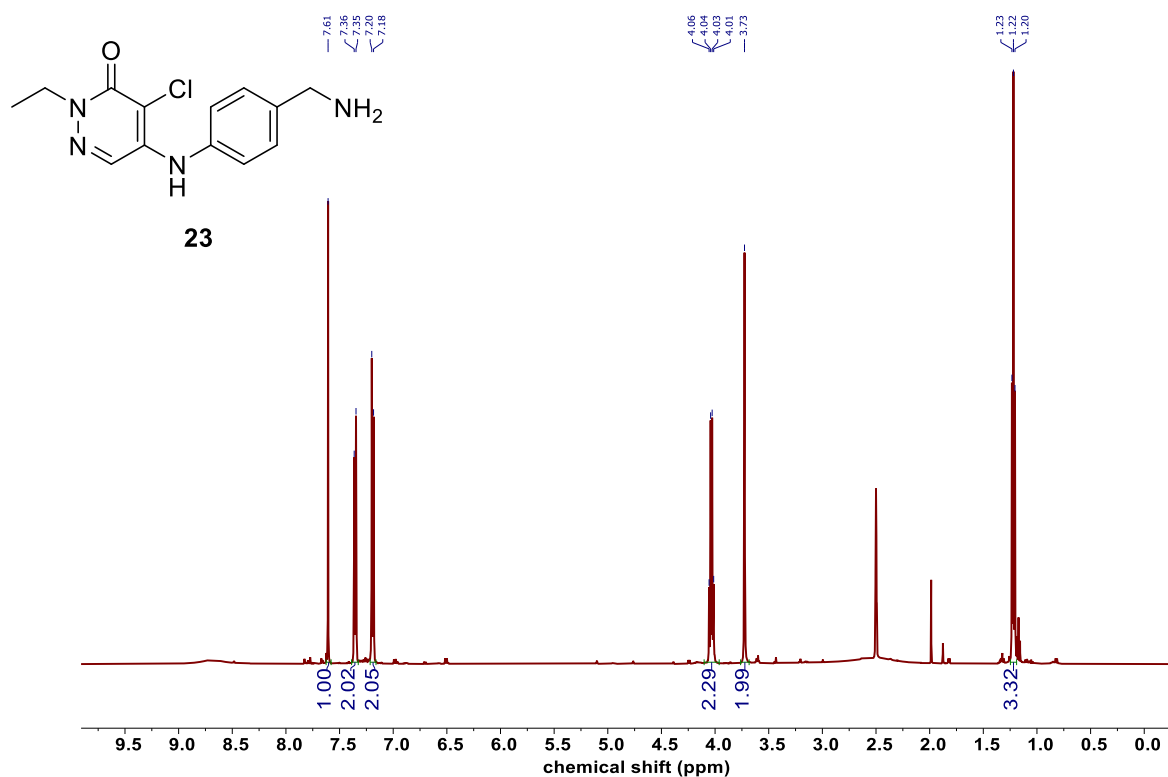
22, ^1H NMR (500 MHz, $\text{DMSO-}d_6$)



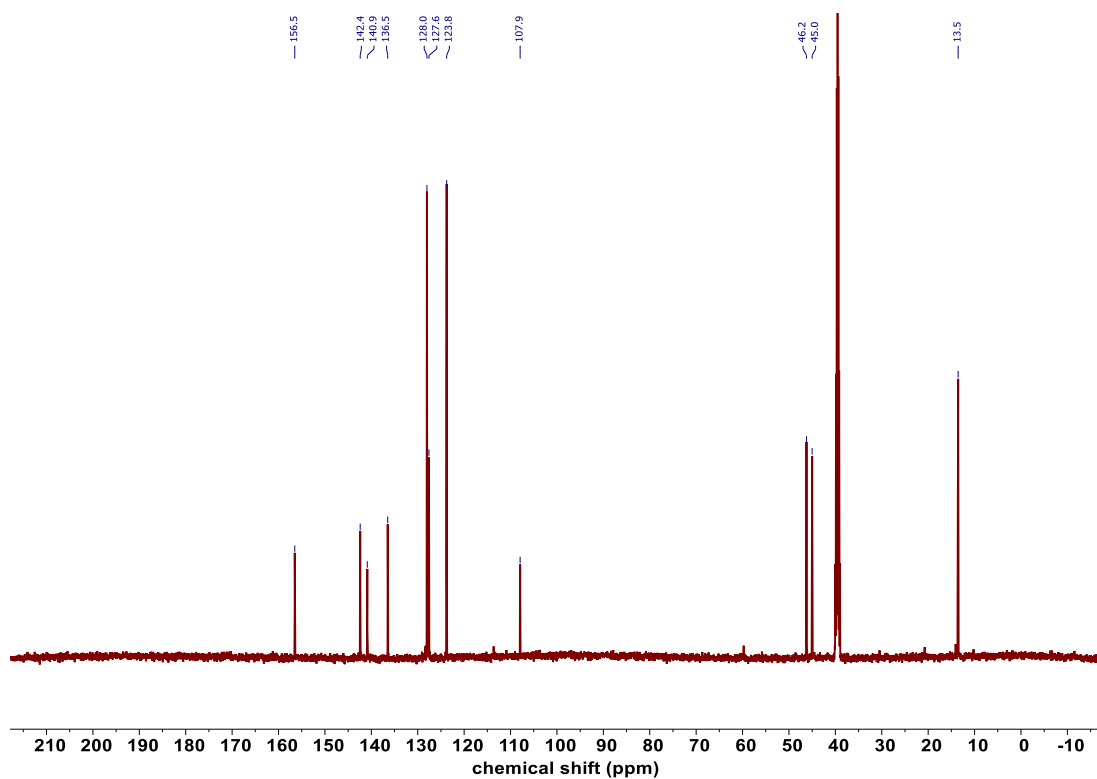
22, ^{13}C NMR (126 MHz, $\text{DMSO-}d_6$)



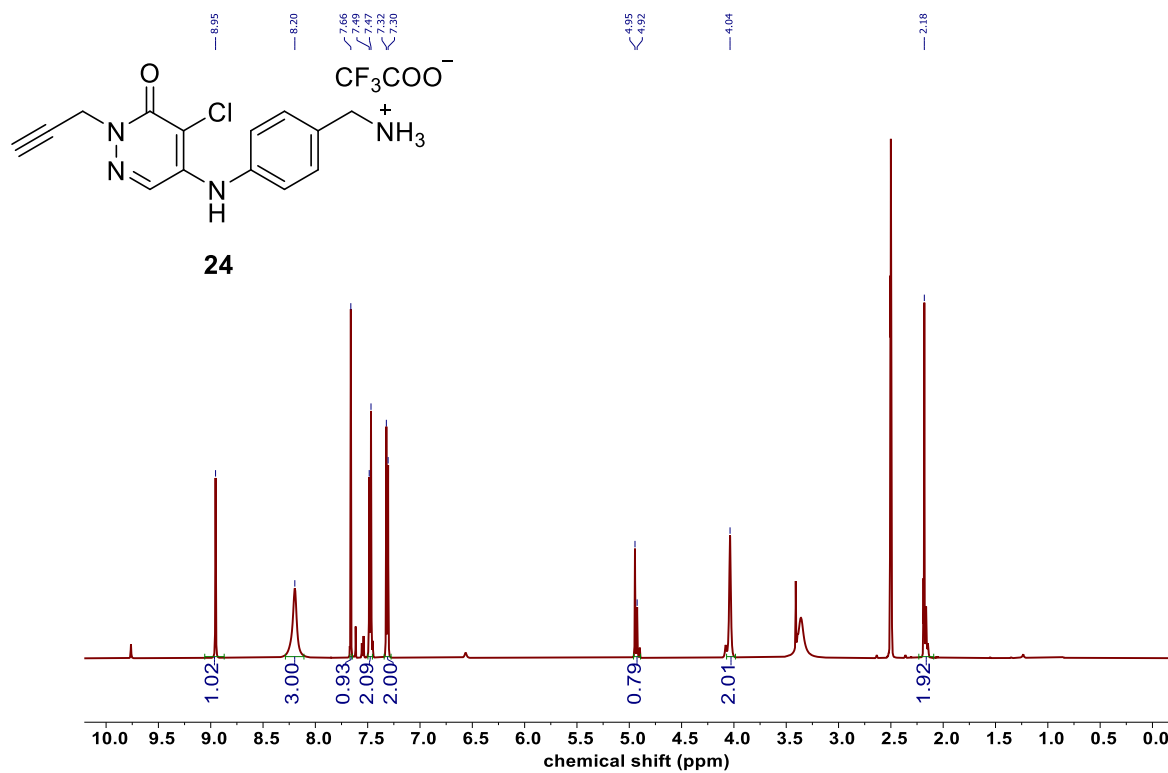
23, ^1H NMR (500 MHz, $\text{DMSO-}d_6$)



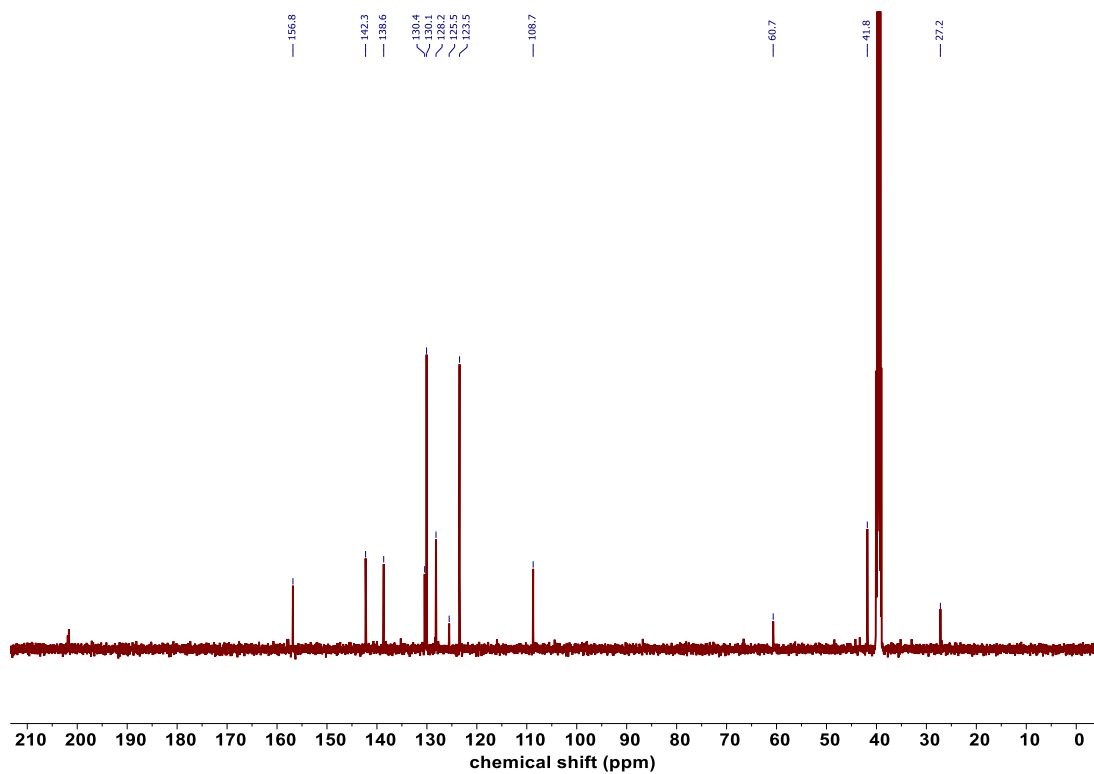
23, ^{13}C NMR (126 MHz, $\text{DMSO-}d_6$)



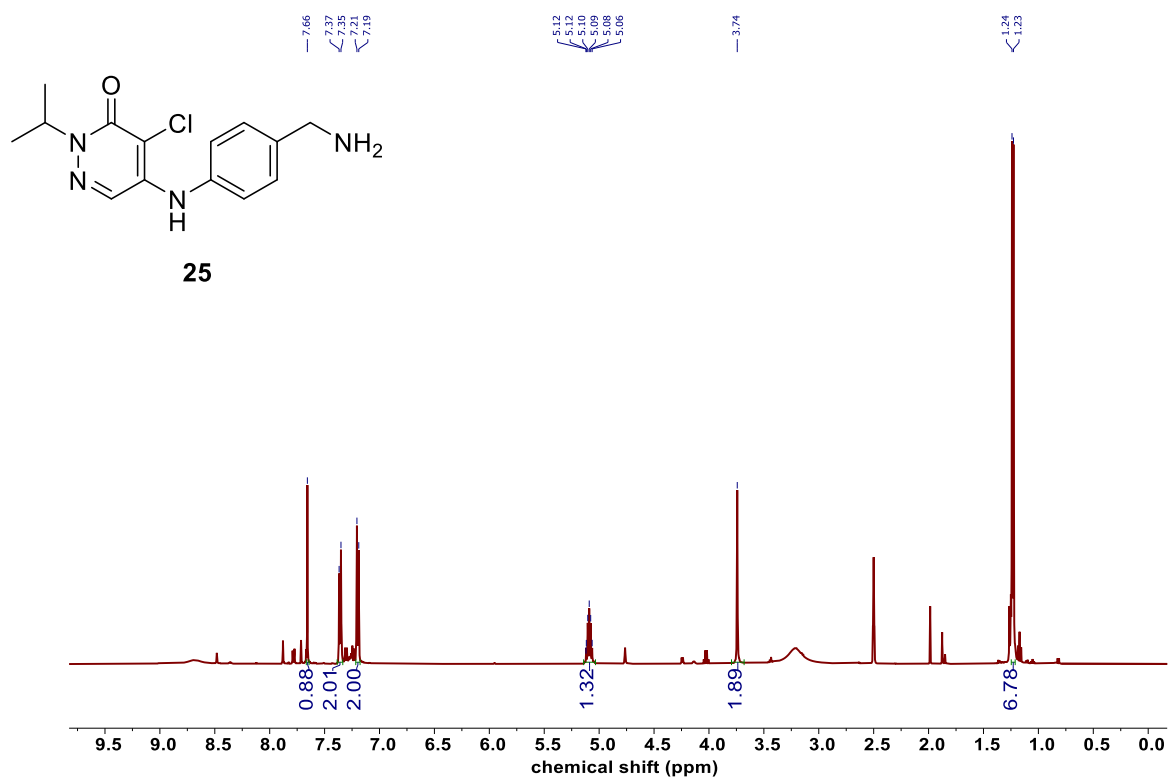
24, ^1H NMR (500 MHz, $\text{DMSO-}d_6$)



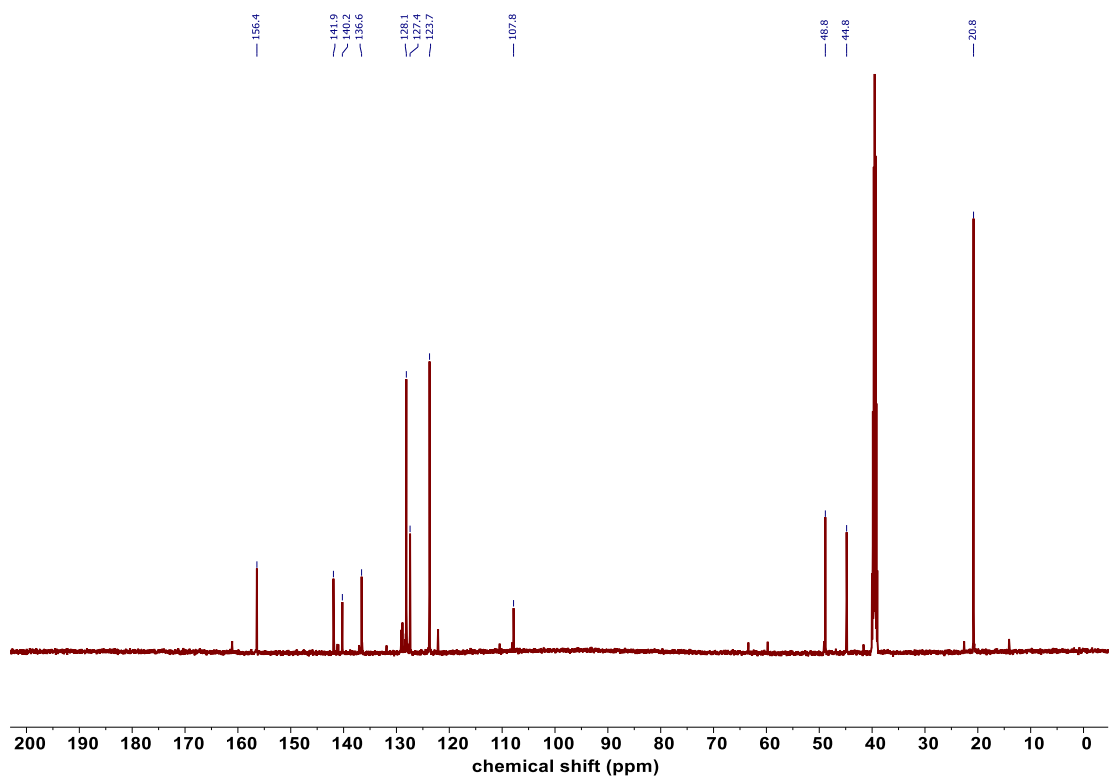
24, ^{13}C NMR (126 MHz, $\text{DMSO-}d_6$)



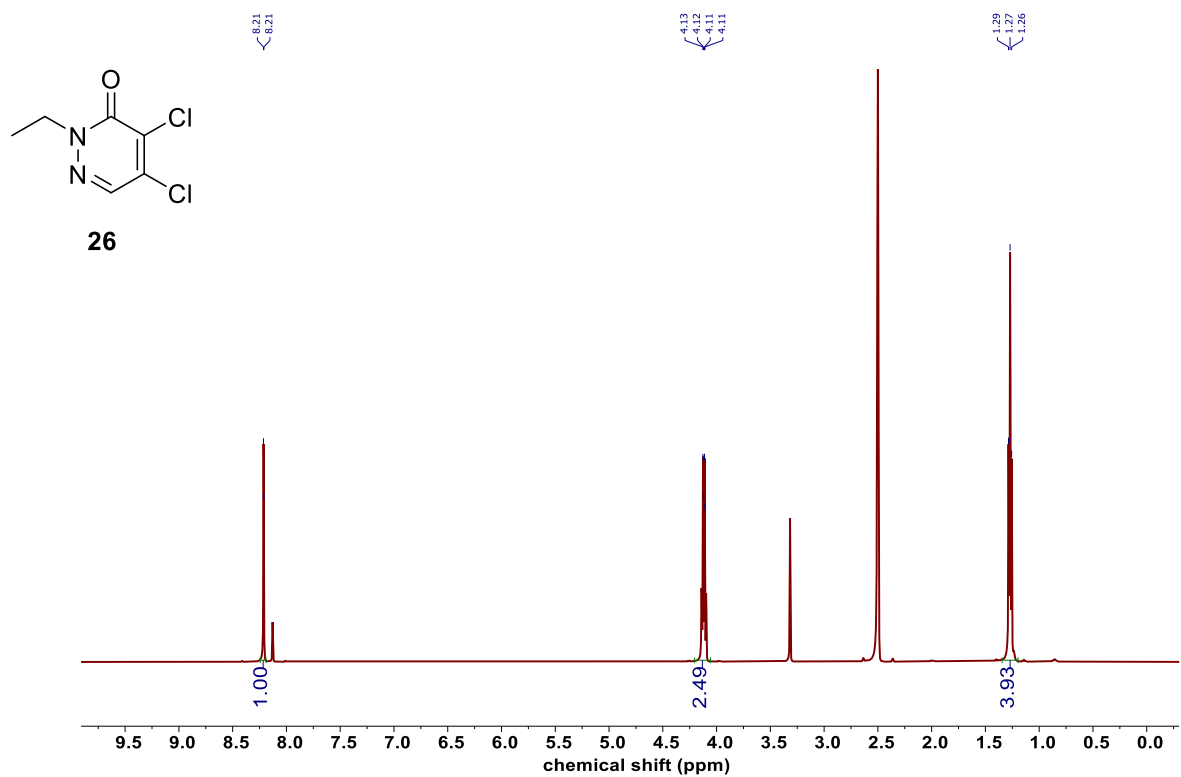
25, ^1H NMR (500 MHz, $\text{DMSO}-d_6$)



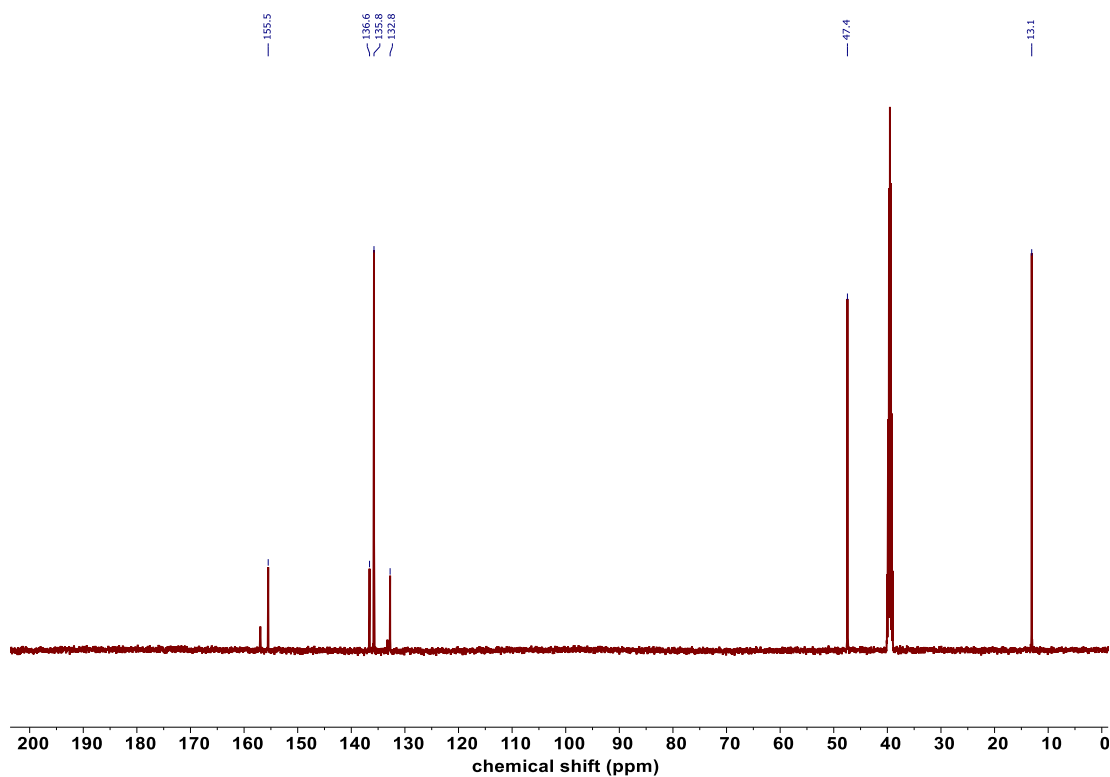
25, ^{13}C NMR (126 MHz, $\text{DMSO}-d_6$)



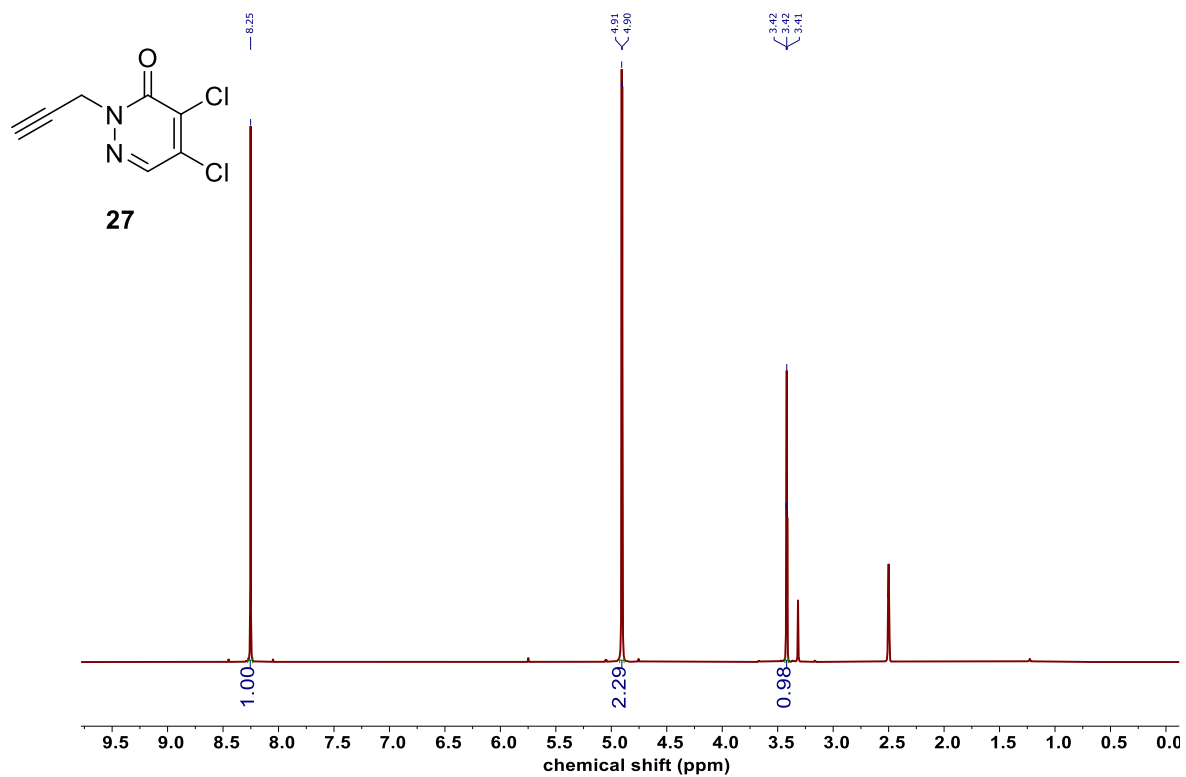
26, ^1H NMR (500 MHz, $\text{DMSO-}d_6$)



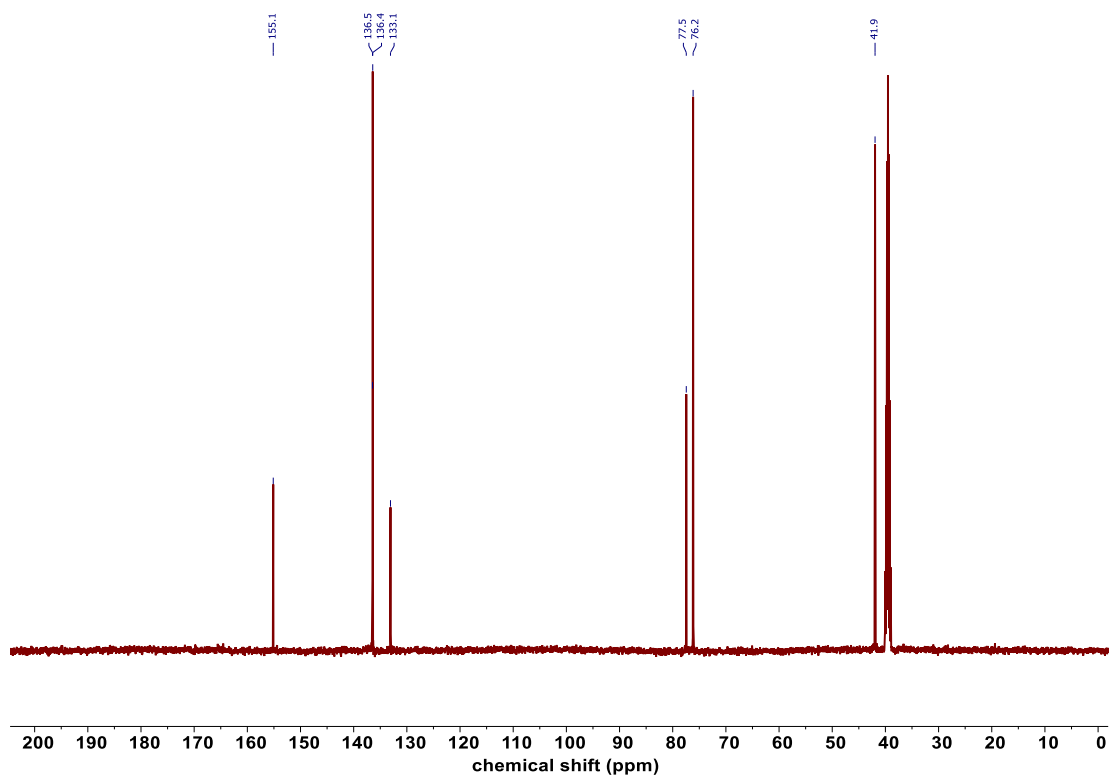
26, ^{13}C NMR (126 MHz, $\text{DMSO-}d_6$)



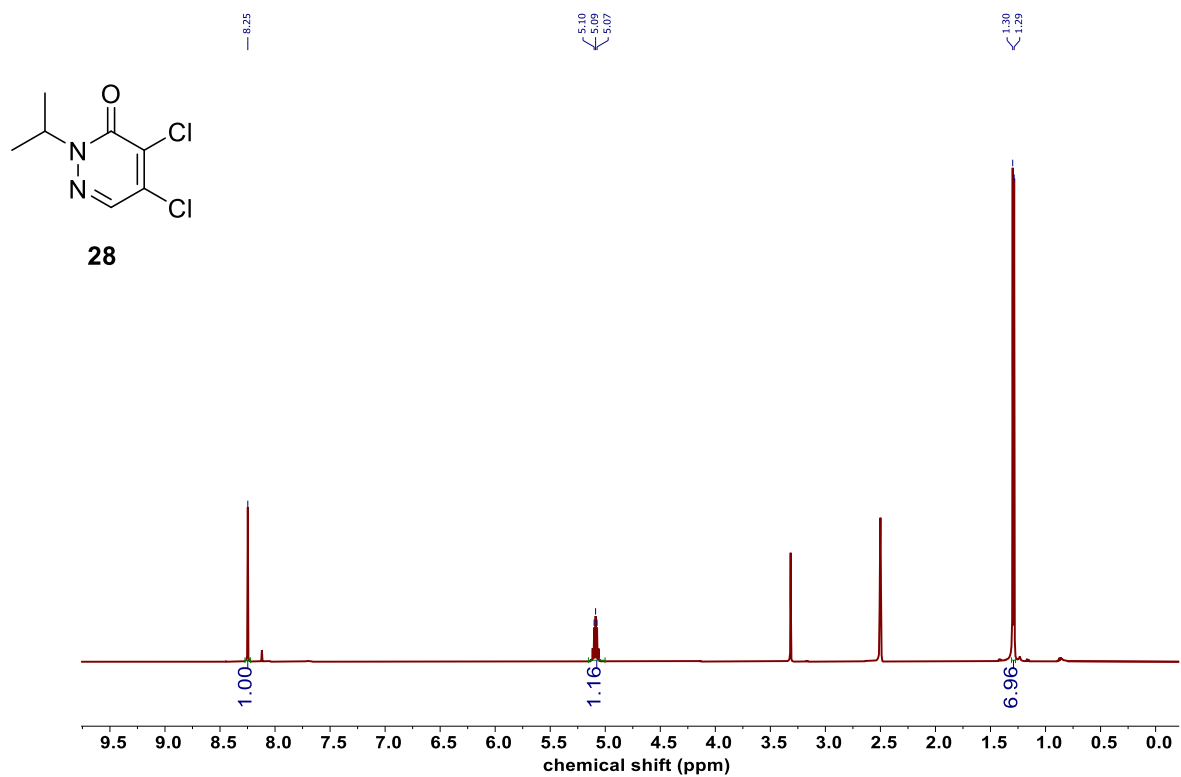
27, ^1H NMR (500 MHz, $\text{DMSO-}d_6$)



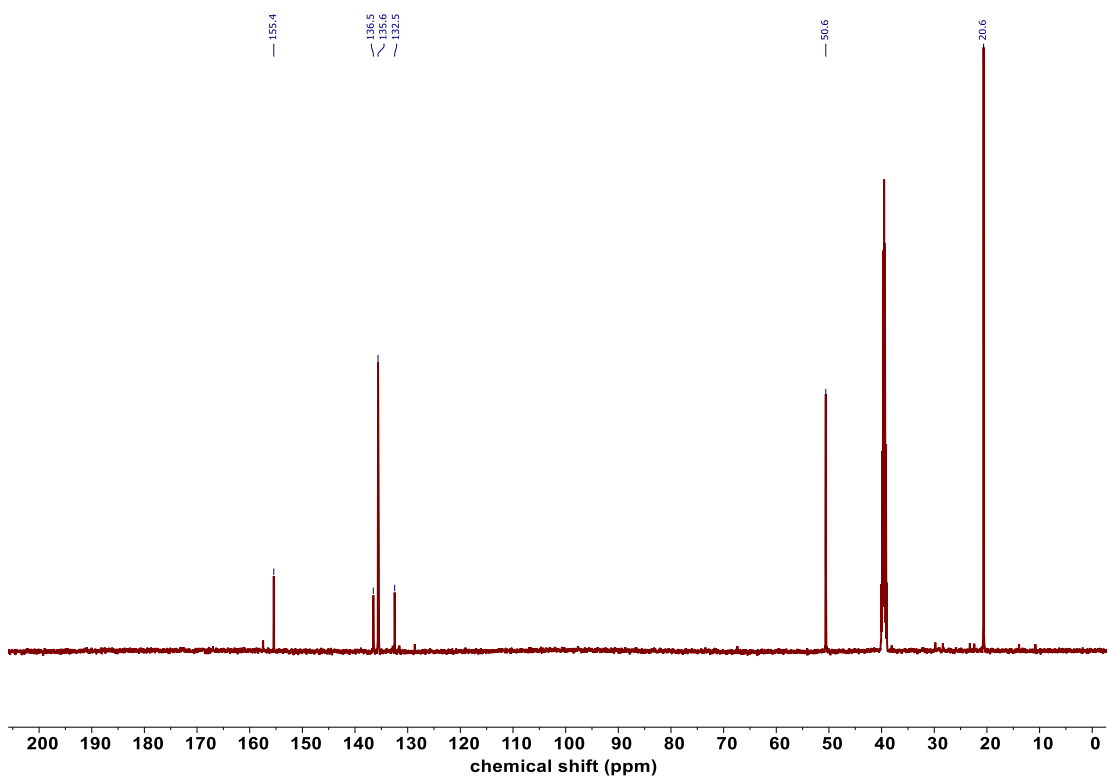
27, ^{13}C NMR (126 MHz, $\text{DMSO-}d_6$)



28, ^1H NMR (500 MHz, $\text{DMSO-}d_6$)



28, ^{13}C NMR (126 MHz, $\text{DMSO-}d_6$)



References

- (1) Mayes, K.; Alkhatib, S. G.; Peterson, K.; Alhazmi, A.; Song, C.; Chan, V.; Blevins, T.; Roberts, M.; Dumur, C. I.; Wang, X.-Y.; Landry, J. W. BPTF Depletion Enhances T-Cell-Mediated Antitumor Immunity. *Cancer Res.* **2016**, *76* (21), 6183–6192.
- (2) Frey, W. D.; Chaudhry, A.; Slepicka, P. F.; Ouellette, A. M.; Kirberger, S. E.; Pomerantz, W. C. K.; Hannon, G. J.; dos Santos, C. O. BPTF Maintains Chromatin Accessibility and the Self-Renewal Capacity of Mammary Gland Stem Cells. *Stem Cell Reports* **2017**, *9* (1), 23–31.